Eur Biophys J (2009) 38:941–960
DOI 10.1007/s00249-009-0475-4

ORIGINAL PAPER

Activation of Bax by joint action of tBid and mitochondrial outer membrane: Monte Carlo simulations

Valery G. Veresov · Alexander I. Davidovskii

Received: 28 February 2009 / Revised: 30 April 2009 / Accepted: 4 May 2009 / Published online: 24 May 2009

Abstract The mitochondrial pathway of apoptosis proceeds when molecules, such as cytochrome *c*, sequestered between the outer and inner mitochondrial membranes are released to the cytosol by mitochondrial outer membrane (MOM) permeabilization. Bax, a member of the Bcl-2 protein family, plays a pivotal role in mitochondrion-mediated apoptosis. In response to apoptotic stimuli, Bax integrates into the MOM, where it mediates the release of cytochrome *c* from the intermembrane space into the cytosol, leading to caspase activation and cell death. The pro-death action of Bax is regulated by interactions with both other prosurvival proteins, such as tBid, and the MOM, but the exact mechanisms remain largely unclear. Here, the mechanisms of integration of Bax into a model membrane mimicking the MOM were studied by Monte Carlo simulations preceded by a computer prediction of the docking of tBid with Bax. A novel model of Bax activation by tBid was predicted by the simulations. In this model, tBid binds to Bax at an interaction site formed by Bax helices α1, α2, α3 and α5 leading, due to interaction of the positively charged N-terminal fragment of tBid with anionic lipid headgroups, to Bax reorientation such that a hydrogen-bonded pair of residues, Asp98 and Ser184, is brought into close proximity with negatively charged lipid headgroups. The interaction with these headgroups destabilizes the hydrogen bond which results in the release of helix α9 from the Bax-binding groove, its insertion into the membrane, followed by insertion into the membrane of the α5–α6 helical hairpin.

Keywords Apoptosis · Bax · tBid · Mitochondria · Monte Carlo simulations

Introduction

In most cells, apoptosis occurs when permeabilization of the mitochondrial outer membrane (MOM) releases apoptogenic proteins, such as cytochrome *c*, from the intermembrane space of mitochondria into the cytosol, which results in the activation of caspases followed by cell destruction (Danial and Korsmeyer 2004; Kroemer et al. 2007). In multicellular organisms, these events, which are critical for cell fate, are controlled by proapoptotic and antiapoptotic members of a large family of proteins known as the Bcl-2 family (Youle and Strasser 2008). The molecular mechanisms of apoptosis regulation by the proteins of the Bcl-2 family are far from being clearly understood. Almost all available hypotheses for this process suggest activation of the Bcl-2 family proapoptotic proteins Bax and/or Bak because their combined loss renders cells resistant to a great variety of apoptotic stimuli (Danial and Korsmeyer 2004). While Bak is constitutively integrated into the MOM, Bax remains, in the absence of an apoptotic stimulus, either as a soluble entity in the cytoplasm or loosely associated with membrane surfaces. It is commonly supposed that following a death signal, cytosolic Bax translocates to mitochondria where it binds to the MOM and undergoes a structural reorganization, which facilitates its insertion into the MOM (Wolter et al. 1997; Goping et al. 1998; Yethon et al. 2003; Linseman et al. 2004). It is widely accepted that the insertion process

Electronic supplementary material The online version of this article (doi:10.1007/s00249-009-0475-4) contains supplementary material, which is available to authorized users.

V. G. Veresov (✉) · A. I. Davidovskii
Department of Cell Biophysics, Institute of Biophysics and Cell Engineering, Academicheskaya St. 27, Minsk 220072, Belarus
e-mail: veres@biobel.bas-net.by

is promoted by proapoptotic BH3-only proteins, such as proteolitically cleaved Bid, tBid, which modifies the conformation of Bax, enabling it to exert its proapoptotic function (Desagher et al. 1999; Eskes et al. 2000; Oh et al. 2006). In the MOM, Bax forms oligomeric pores that allow the release of cytochrome *c* and other proapoptotic factors followed by activation of caspases and cell destruction (Eskes et al. 2000; Wei et al. 2001; Antonsson et al. 2001). Despite extensive study, the precise molecular mechanisms involved remain still largely unresolved. Protein–protein interactions between Bax and other Bcl-2 family proteins as well as between Bax and lipids are key to the regulation of Bax activity. The activated BH3-only proteins, like tBid, and mitochondria-specific lipids (cardiolipins) seem to act jointly to permeabilize the MOM (Lutter et al. 2000; Kuwana et al. 2002; Lovell et al. 2008), but how they achieve this is still not known.

Recent studies with the hydrocarbon-stapled BH3 α-helices of Bid and Bim have demonstrated the direct binding of these helices to Bax and its activation (Walensky et al. 2006; Gavathiotis et al. 2008), whereas experiments using soluble protein domains and peptides that did not undergo such stabilization of α-helicity have failed to demonstrate productive interactions between BH3-only proteins and Bax (Willis et al. 2007). However, in other studies, membrane permeabilization in cells, isolated mitochondria, or liposomes by full-length Bax usually depends upon addition of either a BH3 protein or peptide, while not requiring any artificial reinforcement of their α-helicity (Kuwana et al. 2002, 2005; Yethon et al. 2003; Terrones et al. 2004; Lovell et al. 2008). A crucial difference between these three approaches is the employment in the former of an artificially stabilized helix and inclusion in the latter of a lipid bilayer in the form of a liposome or isolated cellular membrane. Thus, except for the cases with artificially stabilized BH3 peptides, the minimum components required in vitro for membrane permeabilization include Bax, an activator BH3 peptide or protein, and a lipid membrane.

The structure of the water-soluble form of Bax has been solved (Suzuki et al. 2000; Gavathiotis et al. 2008). It resembles that of the pore-forming domains of colicins and diphtheria toxin, where two central hydrophobic α helices are surrounded by a group of amphipathic ones. By analogy with colicins, for which the mechanism of action has been studied in more detail (Parker and Feil 2005), it was proposed that two central α-helices of Bax, α5 and α6, might be responsible for the formation of transmembrane pores (Suzuki et al. 2000). This colicin-like model, which is generally assumed, implies TM-spanning insertion of both α5 and α6 helices for which there is only indirect or incomplete evidence (Nouraini et al. 2000; Heimlich et al. 2004; Garcia-Saez et al. 2004; Franzin et al. 2004; Annis et al. 2005). If the model is valid, an understanding of the physics of the insertion of these helices into the hydrophobic core of the membrane would be especially intriguing because the above segments in Bax contain a significant number of charged residues, which should impose restrictions on a membrane-inserted state (Nouraini et al. 2000).

Bax contains a 21-amino-acid C-terminal hydrophobic segment (helix α9), referred to as a signal-anchor or tail-anchor sequence, that is responsible for the initial targeting and integration of the protein to mitochondria during apoptosis, as deletion of this segment in Bax abrogates its ability to insert into mitochondria during apoptosis (Wolter et al. 1997), while substitution of the segment with that of Bcl-xL abolishes its proapoptotic properties, although without affecting its subcellular localization (Oliver et al. 2000). Ser184 from helix α9 was found to be one of the most important residues in determining Bax subcellular localization and cell death (Nechustan et al. 1999). In particular, while wild-type Bax is located in the cytosol in healthy cells and becomes mitochondrion-bound in cells undergoing apoptosis, the mutation S184K led to a diffuse cytoplasmic localization of Bax even after the cells had received a death signal and protected cells from apoptosis. In contrast, deletion of Ser184 or substitutions Ser184Ala and Ser184Val produced Bax mutants that were constitutively localized in mitochondria even in healthy cells and that were much more toxic than wild-type Bax (Nechustan et al. 1999). Based on the Bax structure in solution (Suzuki et al. 2000), Bax was hypothesized to change its conformation after triggering of apoptosis and to insert helix α9 into the mitochondrial membrane. This hypothesis explains the previous observations of Nechustan et al. (1999), since mutations at the C-termini will impede or enable the interaction of the C-terminal domain with the hydrophobic pocket. To be inserted into the MOM, the hydrogen bond between Ser184 and Asp98 that holds helix α9 within the hydrophobic binding groove on the Bax surface must be disrupted, but how this could be achieved is one of the central questions about mitochondrial apoptosis that remains unanswered.

Characterizing the mechanistic basis for interactions of Bcl-2 family proteins both with membranes and to one another is crucial for understanding apoptosis, but structural studies of these interactions are technically very challenging, and the key details have still not been resolved. For Bax, our present view of its interaction with the mitochondria or with other proteins relies on inferences derived from functional, biochemical, and biophysical data that are insufficient to reproduce the behavior of the system with atomic-resolution details and are often of low reliability (Leber et al. 2007). Because the direct experimental determination of the structures of Bax and its complexes in the membrane environment is likely to be many years

away, computer modeling could make a valuable contribution with a level of detail that is not accessible to experiment and could significantly complement experimental studies. Generally, the most detailed and accurate approach to modeling protein–membrane interactions involves explicit representation of the membrane lipid and water molecules used in molecular dynamics (MD) simulations (reviewed in Ash et al. 2004; Sperotto et al. 2006; Bond and Sansom 2006; Bond et al. 2007). However, all-atom explicit simulations providing the most realism have a prohibitive cost in terms of computing time required for the analysis. In addition, they require laborious procedures to provide information on the thermodynamics of protein insertion into the membrane or of the protein-folding process. A promising alternative approach lies in employment of the Monte Carlo (MC) method with an implicit representation of both the membrane and the solvent. Such an approach, which subsumes the lipid and solvent degrees of freedom into an implicit formulation that captures the average effect, is significantly less computationally expensive than explicit solvent–protein–membrane consideration and, therefore, is able to address questions about structure and function of membrane proteins determined by processes on rather larger time scales.

Here, we report the results of a combined application of the Metropolis Monte Carlo approach and of computer prediction of the docking of tBid with Bax to the analysis of the interactions among Bax, tBid, and a model lipid membrane.

Materials and methods

The membrane model

It was suggested that Bax binds to the MOM at the region of mitochondrial contact sites (Kuwana et al. 2002; Capano and Crompton 2002). The implicit membrane model for the MOM contact site region was used. In this model, the membrane was represented as a slab with the plane of smeared negative charge (corresponding to the position of the centers of headgroups of cardiolipins) offset inward the membrane from its surface by 4 Å in accordance with the data on the thickness of headgroup region (Peitzsch et al. 1995). The membrane slab and the plane of smeared negative charge were disposed parallel to the *xy*-plane. The data on the lipid composition of the outer leaflet of the contact sites (Ardail et al. 1990; Lutter et al. 2000) were used for the calculation of the effective surface charge density σ of the model membrane, which was assumed to be the sum of negative surface charge density due to acidic lipids in the membrane and a positive surface charge density due to membrane-adsorbed cations.

The protein model

The total free energy of a protein (G_{tot}) was taken in the form:

$$\begin{aligned} G_{\mathrm{tot}} &= G_{\mathrm{ECEPP}/2/3} + G_{\mathrm{env}} \\ &= G_{\mathrm{ECEPP}/2/3} + G_{\mathrm{solv}} + G_{\mathrm{qE,\,m}} + G_{\mathrm{env,\,pert}} \end{aligned} \quad (1)$$

The term $G_{\mathrm{ECEPP}/2/3}$ includes van der Waals, torsion, electrostatic, and H-bond contributions to intraprotein potential energy taken in the ECEPP2/ECEPP3 protein force-field parameterization (Dunfield et al. 1978; Némethy et al. 1983, 1992). G_{env} describes the interaction of the protein with the environment, which can be decomposed into the sum of contributions involving free energy of solvation, G_{solv}, energy of electrostatic interaction with the membrane, $G_{\mathrm{qE,m}}$, and the energy of the environment perturbation, $G_{\mathrm{env,pert}}$.

The following expressions were used for G_{solv} and $G_{\mathrm{env,pert}}$ during simulations [see Veresov and Davidovskii (2007) and Supplementary Data SA in the Supplementary Material file]:

$$G_{\mathrm{solv}} = G_{\mathrm{solv}}^{\mathrm{wat}} + (G_{\mathrm{solv}} - G_{\mathrm{solv}}^{\mathrm{wat}}) = G_{\mathrm{solv}}^{\mathrm{wat}} + \Delta G_{\mathrm{solv}}, \quad (2a)$$

$$\begin{aligned} G_{\mathrm{env,\,pert}} &= G_{\mathrm{env,\,pert}}^{\mathrm{wat}} + (G_{\mathrm{env,\,pert}} - G_{\mathrm{env,\,pert}}^{\mathrm{wat}}) \\ &= G_{\mathrm{env,\,pert}}^{\mathrm{wat}} + \Delta G_{\mathrm{env,\,pert}}, \end{aligned} \quad (3a)$$

where ΔG_{solv} and $\Delta G_{\mathrm{env,pert}}$ are given by

$$\begin{aligned} \Delta G_{\mathrm{solv}} &= \sum_{j=1}^{N} (G_{\mathrm{solv},j}^{\mathrm{m}} - G_{\mathrm{solv},j}^{\mathrm{wat}})(1 - g(z_j)) \\ &= \sum_{jr=1}^{N_{\mathrm{res}}} (s_{jr}\mathrm{rASA}_{s,jr}\eta(z_{jr,\mathrm{Cb}}) + c_{jr}\mathrm{rASA}_{b,jr}\eta(z_{jr,\mathrm{Ca}})), \end{aligned} \quad (2b)$$

$$\Delta G_{\mathrm{env,\,pert}} = \sum_{jr}^{N_{\mathrm{res}}} p_{jr} = \sum_{jr}^{N_{\mathrm{res}}} (G_{\mathrm{pert},jr}^{\mathrm{m}} - G_{\mathrm{pert},jr}^{\mathrm{wat}}), \quad (3b)$$

where $G_{\mathrm{solv}}^{\mathrm{wat}}$ is the solvation free energy of the protein in water, $G_{\mathrm{solv},j}^{\mathrm{wat}}$ and $G_{\mathrm{solv},j}^{\mathrm{m}}$ are the solvation free energies of the protein atom j in water and in the membrane, respectively. $G_{\mathrm{pert},jr}^{\mathrm{m}}$ and $G_{\mathrm{pert},jr}^{\mathrm{wat}}$ are the energies of perturbation by the residue jr of the membrane and the water phases, respectively. The sum of differences $\Delta G_{\mathrm{solv},j} = G_{\mathrm{solv},j}^{\mathrm{m}} - G_{\mathrm{solv},j}^{\mathrm{wat}}$ and $\Delta G_{\mathrm{pert},j} = G_{\mathrm{pert},j}^{\mathrm{m}} - G_{\mathrm{pert},j}^{\mathrm{wat}}$ defines the free energy of the atom j transfer from water to the membrane core, where $G_{\mathrm{pert},j}^{\mathrm{m}}$ and $G_{\mathrm{pert},j}^{\mathrm{wat}}$are the energies of perturbation by the atom j of the membrane and the water phases, respectively. s_{jr} and c_{jr} are the average transfer free energies of a side chain and a backbone chain of the residue jr from water to membrane core due to desolvation, $\mathrm{rASA}_{s,jr}$ and $\mathrm{rASA}_{b,jr}$ are relative accessible surface areas related to those of fully unfolded states for side chains and backbone chains, respectively; the subscripts (jr,Cb) and (jr,Ca) denote

C_β- and C_α-atoms of the residue jr, respectively. $g(z)$ in Eq. 2b is a sigmoid function that was introduced to describe the fractional water content (the hydrophilicity of the environment for each atom) as the function of the distance $z_j - z_w$ from the interfacial membrane plane located at z_w (Baumgaertner 1996; Kessel et al. 2003; Shental-Bechor et al. 2007; Veresov and Davidovskii 2007):

$$g(z_j) = 1/(1 + \exp[-(z_j - z_w)/\lambda]), \quad (4)$$

where the decay length λ was taken as equal to 2 Å; $\eta(z)$ in the Eq. 2b stands for $1-g(z)$.

The free energies of partitioning s_{jr}, c_{jr}, p_{jr} of amino acids from water into the cell membrane are among the most critical parameters for predicting membrane protein stability and configuration. A considerable number of amino acid hydropathy scales have been experimentally and computationally devised to evaluate the free energy of partitioning of amino acids from water into the hydrophobic core of lipid membranes [reviewed and discussed in White and Wimley (1999), Kessel and Ben-Tal (2002), White (2007), Wolfenden (2007) and MacCallum et al. (2007)]. Upon obtaining these scales experimentally, the partitioning of amino acids into a membrane has been approximated by partitioning in hydrophobic solvents, typically in either *n*-octanol (low-polarity) or cyclohexane (almost ideally nonpolar). The hydrophobicities of real biological membranes are thought to lie between the hydrophobicities of these two solvents (Wolfenden 2007; MacCallum et al. 2007), and therefore it is necessary to interpolate between octanol-like and cyclohexane-like scales to describe the membrane–protein interactions properly. Because precise data on the polarity of the hydrophobic part of the MOM are lacking, it was decided to use three types of scales, and in particular, the Wimley–White (WW) water-to-octanol scale (White and Wimley 1999), Kessel-Ben-Tal (KBT) cyclohexane-like computationally derived scale (Sitkoff et al. 1996; Kessel and Ben-Tal 2002), and the hybrid KBT-LysWW scale where the value of 7.4 kcal/mol for Lys in the KBT scale is replaced by the 2.71 kcal/mol value from the WW scale. The KBT scale was selected among other cyclohexane-like scales as the only scale that contains, though not directly for the MOM, both the contribution from membrane perturbations by residues incorporated into the membrane and the free-energy penalty of inserting the helix backbone into the membrane. The use of the KBT-LysWW scale in our simulations can be justified by the belief that when lysines insert into the bilayer interior they are accompanied either by a few water molecules (Jayasinghe et al. 2001) or by lipid phosphate headgroups (Tang et al. 2007) thus raising the local polarity of the bilayer interior around lysine side chains to about that of octanol.

To account for either the membrane interface or the membrane hydrophobic core preferences of different amino acid residues, three scales, WW scale, KBT scale, and KBT-LysWW scale, were combined with the POPC (palmitoyloleoylphosphocholine) interface scale of Wimley and White (IFWW) (White and Wimley 1999) leading to three combined scales, WW-IFWW, KBT-IFWW, and KBT-LysWW-IFWW. To achieve this, a z-dependence of s_{jr} in the Eq. 2b was introduced by the expression:

$$\begin{aligned} s_{jr} &= s_{jr,\mathrm{hc}}(1 - (1 - r)\exp(z_j - z_w)), & z_w > z_j \\ s_{jr} &= s_{jr,\mathrm{if}}, & z_w \le z_j \end{aligned} \quad (5)$$

where $s_{jr,\mathrm{hc}}$ is the free energy of the transfer of the residue jr from water to the hydrophobic core of the membrane, $s_{jr,\mathrm{if}}$ is the free energy of transfer of the residue from water to the POPC interface, r stands for $r = s_{jr}/s_{jr,\mathrm{hc}}$. ASAs in Eq. 2b were determined by the program GETAREA (Fraczkiewicz and Braun 1998).

The term $G_{\mathrm{qE,m}}$ of Eq. 1 accounts for the electrostatic interaction energy of the protein with the membrane. It was calculated using the Gouy-Chapman-Stern theory for protein atoms in solution and "constant field approximation" for protein atoms within the membrane as described in Veresov and Davidovskii (2007) and Supplementary Material Section SB.

General strategy for the analysis of Bax integration into the MOM

Because a straightforward sampling of the full configurational space of the protein is impractical, experimentally based structural constraints as well as physical and evolutionary considerations were used to reduce the conformational space to be searched (hereafter the term "configuration" will be used to mean the protein conformation together with the spatial arrangement of the protein as a whole with respect to the membrane). For this purpose, the process of integration of Bax into the MOM preceding the oligomerization was divided, on the basis of a number of experimental data, into four stages with four different procedures for conformational space reductions. These stages were (1) translocation of the protein from the solution to the membrane, (2) the insertion of helix α9 into the membrane, (3) the insertion of hairpin α5–α6 into the membrane, and (4) a stage of refinement. The main motive for such a division was an efficient constraining of the conformational space to be sampled using experimental data and experimentally based guesses about Bax intermediate structures or Bax structural rearrangements within each of these stages. The following experimental data

underlay the constraints set on the conformation space to be explored: (1) the absence of significant conformational changes of Bax in solution (in the cytosol) (Suzuki et al. 2000), (2) the initial binding of Bax to the MOM occurs via its C-terminal "tail-anchor," helix (α9) (Wolter et al. 1997; Goping et al. 1998; Nechustan et al. 1999; Suzuki et al. 2000; Annis et al. 2005), (3) Bax also inserts "pore domain" (helices α5–α6, α5–α6-hairpin) and this insertion into the membrane occurs after insertion of the helix α9 and prior to Bax oligomerization and membrane permeabilization (Heimlich et al. 2004; Garcia-Saez et al. 2004; Annis et al. 2005), (4) the unfolding of the protein occurs mainly in the regions of low polarity either on or near the surface of the membrane or within the membrane (Wolter et al. 1997; Suzuki et al. 2000; Yethon et al. 2003; Terrones et al. 2004; Garcia-Saez et al. 2004; Annis et al. 2005) where the stabilization of intrahelical hydrogen bonds, due to the low polarity of the medium, can be expected. In accordance with point (4), it was suggested that the conformational rearrangements of Bax near or within the membrane occur mainly via the changes of the dihedral angles of interhelical loops while the helices themselves remain essentially unchanged.

The experimental data indicate that the insertion of helix α9 into the MOM requires the direct participation of tBid. Based on the results of Bax activation by BH3 peptides of Bcl-2 family proteins, the hypothesis that the disengagement of helix α9 from the Bax hydrophobic groove occurs due to a direct displacement of this helix by the BH3 domain of tBid has been a prevailing view in recent years (Kuwana et al. 2005; Walensky et al. 2006). Quite recently, this hypothesis was called into serious question by NMR data showing that Bim BH3 peptide does not bind to Bax at its canonical hydrophobic groove (Gavathiotis et al. 2008). We hypothesized that direct interaction of tBid with Bax results, due to electrostatic interaction of positively charged tBid with the anionic MOM, in such a displacement of Bax whereby hydrogen-bonded Asp98 and Ser184 of Bax are brought into proximity with the negatively charged cardiolipin heads of the MOM. In this case, the electrostatic interactions between Asp98 and anionic cardiolipin heads and between Ser184 and the polar medium of the headgroup region of the MOM would be expected to displace the energy balance among hydrophobic, electrostatic, and elastic interactions of the helix α9 with the membrane and the Bax binding groove in favor of the helix intramembrane location preceded by the disruption of the hydrogen bond.

To test this hypothesis and elucidate the mechanisms of Bax integration into the MOM as well as to obtain the 3D structure of Bax integrated into the MOM, six types of Monte Carlo simulations with six different types of initial configurations of the protein (shown in Fig. 1c) were performed.

When carrying out *type I* simulations, the backbone dihedral angles of Bax were fixed at their solution values from the NMR structure obtained by Suzuki et al. (2000), while external rigid body translational and rotational motions were allowed. The goal of the simulations of this type was to analyze the behavior of Bax monomer in the cytosol and detect the lowest-energy arrangement of the protein relative to the membrane in healthy cells.

Upon applying *type II* simulations, the lowest-energy configuration from the preceding type of simulation was used as the initial one. To reduce the computing time of these CPU-intensive simulations, a three-stage simulation protocol was used in this case that was based on the following considerations. The residues Gly156 and Gly 157 within loop L7–8 between helices α7 and α8, as well as Gly166 within loop L8–9, do not contain side chains, and therefore are expected to be highly rotatable. Besides, these residues, together with the adjacent Gln155, Phe165, and Thr167, are highly conserved between all known Bax types. Based on these considerations and the experimental data indicating that the insertion of helix α9 into the MOM occurs largely autonomously from the rest of the protein (Annis et al. 2005) and is fast (Nechustan et al. 1999), the residues Gln155, Gly156, Gly157 and Phe165, Gly166, Thr167 were suggested to form two hinge groups that make the main contribution to the release of helix α9 from the Bax binding pocket. Therefore, only the dihedral angles of these six residues were allowed to vary at the first stage of the type II simulations. At the second stage of the type II simulations, all dihedrals of the residues of the loops L6–7, L7–8, and L8–9 were allowed to vary. The cases with Ser (wild-type case), Ala, Val, Asp, and Lys at the residue 184 position were analyzed. At the third stage of the type II simulations, that of refinement, all dihedrals were allowed to vary, while external rigid body translational and rotational motions were ignored. At this stage, the protein was subjected to conjugate gradient minimization. These mutants were selected for examination because the mutations at position 184 are thought to be critical for the insertion of helix α9 into the membrane (Nechustan et al. 1999) and because the data on the insertion of helix α9 of these mutants into the MOM are available from experiment (Nechustan et al. 1999) and therefore can be used for the calibration of parameters of the model and its verification. To eliminate sterically inconsistent conformations when using the NMR structure of wild-type Bax (Suzuki et al. 2000) with Ser 184 substituted by Ala, Val, Asp, or Lys, the mutant structures were subjected to conjugate gradient minimization prior to MC runs.

With *type III* simulations, the spatial arrangement of the rigid complex tBid–Bax was studied. In this case the 3D-structure of the rigid complex tBid–Bax was predicted by the program Hex (Ritchie and Kemp 2000) with shape

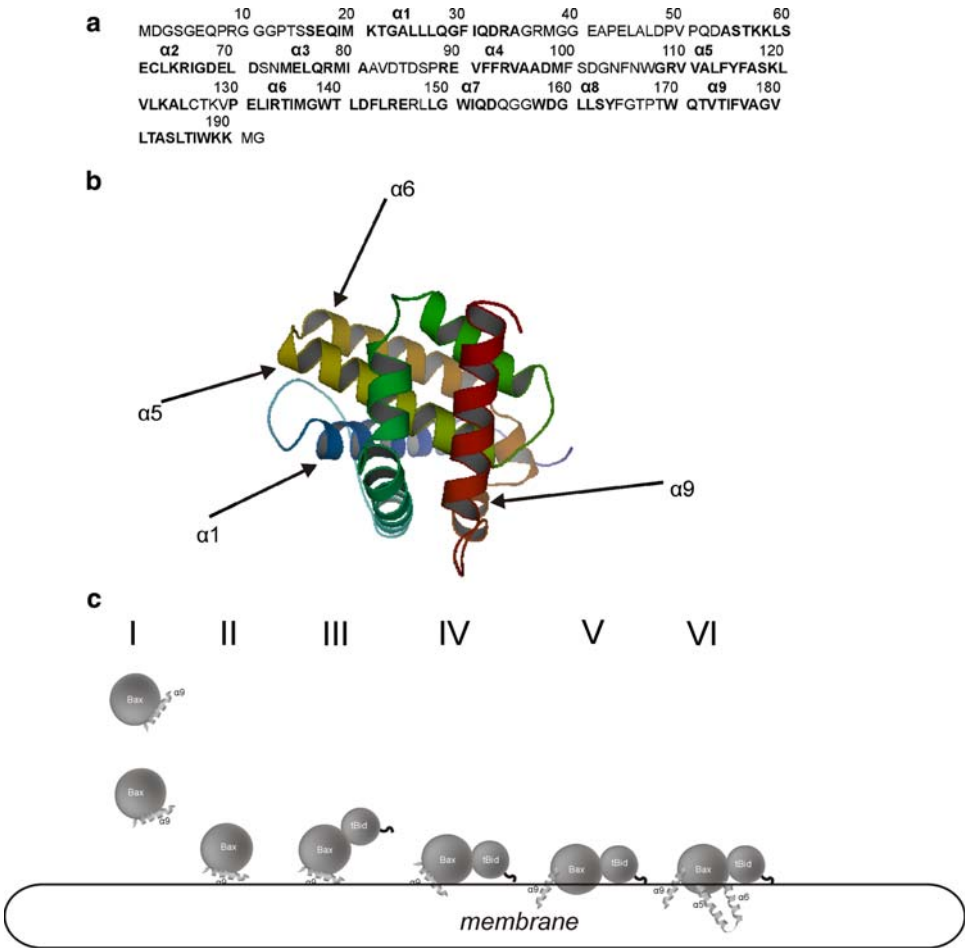

Fig. 1 The amino acid sequence of Bax_human (**a**), the 3D PDB structure of Bax (Suzuki et al. 2000) (PDB accession code 1f16) (**b**), and six initial configurations of Bax used in the simulations (**c**). The starting configurations of type I correspond to the NMR conformation of Suzuki et al. (Suzuki et al. 2000) with different orientations relative to the membrane. The starting configuration of type III corresponds to the tBid–Bax dimer with Bax configuration identical to the lowest-energy configuration of Bax monomer relative to the model membrane. The starting configurations of type II and of type IV are the lowest-energy configurations from the type I and III simulations, respectively. The starting configuration of type V is the lowest-energy configuration of type IV simulations with helix α9 inserted. The starting configuration of type VI is the lowest-energy configuration of type V simulations with helices α5, α6, and α9 inserted. Helices in **a** are depicted in *bold*

plus electrostatics correlations. The best scored complex was submitted to simulations with the initial configuration whereby the configuration of Bax was identical to the lowest-energy one from the simulations of the first type. In the type III simulations, the dihedrals of the tBid–Bax complex other than those of the N-terminal segment preceding the first tBid helix were fixed. In doing this, we were guided by the assumption that the loop preceding the first tBid helix could have different conformations when in full Bid and truncated Bid, tBid.

With *type IV* simulations, only wild-type Bax behavior was studied. In this case, the initial configuration was the lowest-energy one taken from the type III simulations. A three-stage simulation protocol similar to that used with the type II simulations was applied in this case as well.

Type V simulations were carried out only for wild-type Bax starting from the lowest-energy configuration of the type IV simulations. Because this configuration was found to be such (see "Results") that helix α9 was inserted into the membrane, thus clearing the way for the release of hairpin α5–α6 from the hydrophobic core of the protein and towards its insertion into the membrane, it was suggested that the experimentally observed fast insertion of helices α5 and α6 into the membrane performs, at least initially, without any alterations of the protein part involving helices α1–α4. Based on the latter suggestion and taking the shortness of the loops between helices α5 and α6 (L 5–6), and between helices α7 and α8 (L 7–8) into account, only variations of dihedral angles of the residues within the loops between helices 4 and 5 (L 4–5), 7 and 8 (L 7–8), and 8 and 9 (L 8–9) were allowed during the type V simulations.

When performing *type VI* simulations, a three-stage procedure was used with the lowest-energy configuration of the type V simulations taken as the initial one. The residues Gly3, Ser4, Gly5, Gly10, Gly11, Gly12, Gly39, Gly40, Ser101, Asp102, Gly103, Asn104, Gln155, Gly156, Gly157, Phe165, Gly166, and Thr167 either do not have side chains or their side chains are short or these residues are adjacent to those with no side chains. In addition, these residues are highly conserved across all known Bax types. Therefore, these residues were assumed to form hinge groups. With this assumption, all dihedral angles, except those of these residues, were kept fixed at the first stage of the type VI simulations. At the second stage, the dihedral angles within all loops between helices were allowed to

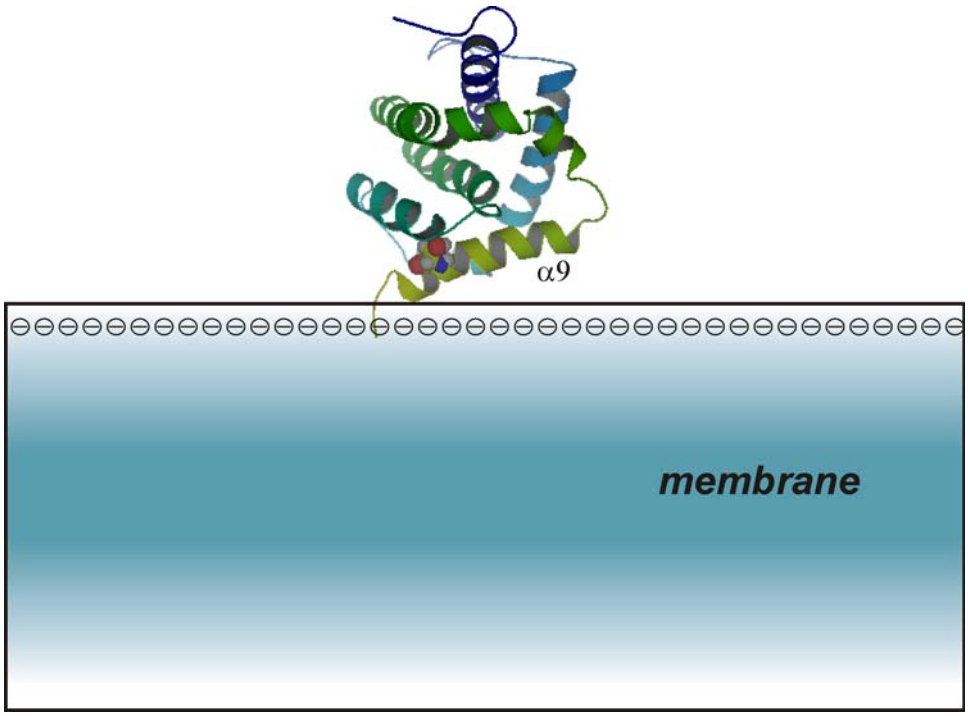

Fig. 2 The 3D structure of a completely folded Bax monomer in its lowest-energy configuration. The α9 helix is depicted in *light green*. The residues Asp98 and Ser184, which form hydrogen bonds, are shown *space-filled*. The *circles with minus signs* inside them represent the plane of the negative surface charge of the membrane. The membrane hydrophobicity profile is color-coded so that *dark blue* represents the most highly hydrophobic region of the lipid chains, progressively *paler tints of blue* correspond to a progressive decrease in hydrophobicity, and the aqueous phase is *white*

vary. At the third stage, the lowest-energy configuration obtained at the second stage was taken as the initial one, and Bax was subjected to conjugate gradient minimization with all dihedral angles of Bax allowed to vary, but ignoring external rigid body translations and rotations.

The generation of sequences of configurations

When performing simulations of types I–VI, Monte Carlo configurational searches in the space of non-fixed generalized coordinates were carried out. Aside from non-fixed dihedral angles, these generalized coordinates included Euler angles and the coordinates of C_α atom of the first N-terminus peptide unit, describing the localization of the protein as a whole relative to the membrane (Veresov and Davidovskii 2007). With these simulations, we followed standard Metropolis MC criteria of the acceptance of each move in sampling the configurational space of the protein. New configurations were generated by simultaneously perturbing the generalized coordinates [a detailed description of the sampling protocol is available in Veresov and Davidovskii (2007) and Supplementary file SC]. When type I simulations were carried out, the dihedral angles both of the backbone and of the side chains were fixed. Generally, the simulations of types I and III, as well as of the first stages of types II and IV–VI with partially fixed dihedral angles of interhelical residues, included 100,000-200,000 full cycles for each starting structure. At the second stages of the simulations of types II and IV–VI, 5,000 full MC cycles were performed with no dihedrals of interhelical loops being fixed. At the third stages of the simulations of types II and IV–VI, conjugate gradient minimizations were carried out on the space of all dihedral angles, with Euler angles being fixed.

Results

Nonactivated Bax binds weakly to the model membrane mimicking the MOM

To reproduce the behavior of cytosolic Bax in healthy (nonapoptotic) cells, five independent runs of 200,000 MC cycles each of the type I simulations for the completely folded Bax [the NMR-structure from Suzuki et al. (2000)] with five different initial distances from the membrane and different initial orientations of the protein were carried out under conditions when all dihedral angles were maintained fixed, while external rigid body rotational and translational motions were allowed. In all cases, starting from an arbitrary aqueous phase configuration, Bax adsorbed to the membrane in the head region with its most positively charged side (the side of the location of the helix α9) oriented towards the membrane. The RMSDs of Euler angles and of the protein distance to the membrane from those of the lowest-energy (−1.8 kcal/mol for the interaction with the membrane) configuration (shown in Fig. 2) averaged over last 50,000 MC cycles were less than 12° and 3 Å, respectively. Figure 2 shows that while Lys189 and Lys190 lie close to the plane of negative charge in the

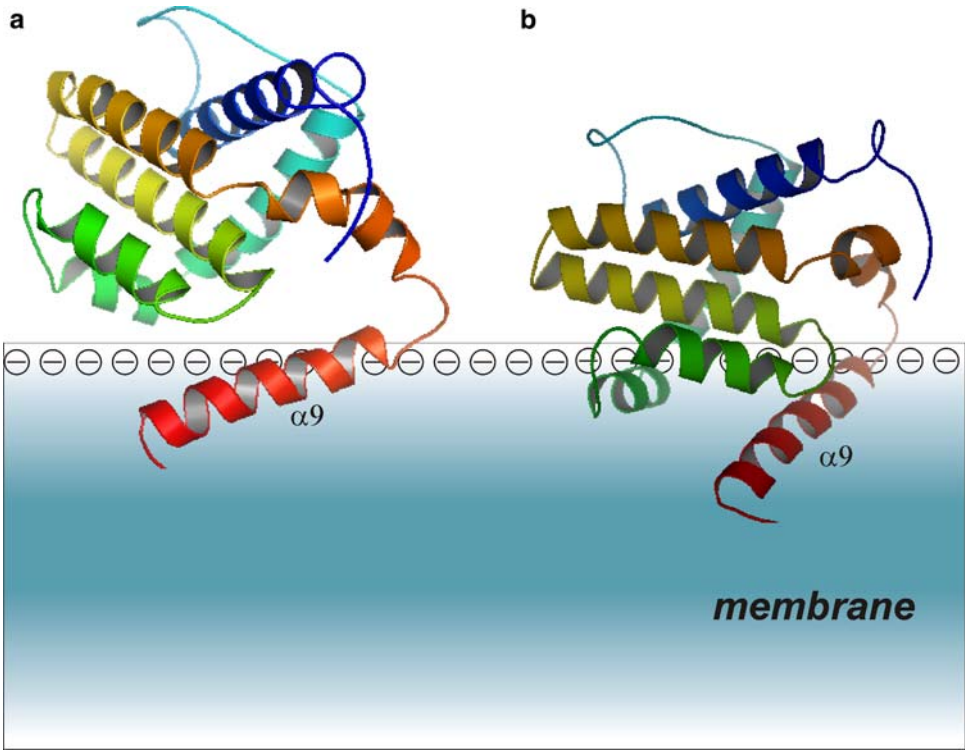

Fig. 3 The lowest-energy configurations of the type II simulations for the mutants Bax-S184A (**a**) and Bax-S184V (**b**). The membrane hydrophobicity profile and the membrane surface charge are represented using the scheme of Fig. 2

lowest-energy state, the hydrogen-bonded pair of residues Asp98-Ser184 is well off the membrane. These results show that Bax prefers to be weakly bound to the model membrane mimicking the MOM without any external activation.

The membrane-driven behavior of helix α9 in the cases of wild-type Bax and mutants Bax-Ser184Ala, Bax-Ser184 Val, Bax-Ser184Asp, and Bax-Ser184Lys

The analyses of unfolding of helix α9 and its insertion into the membrane via the use of the type II simulations were performed for the cases of wild-type Bax (wt-Bax) and Bax-mutants Bax-S184A, Bax-S184V, Bax-S184D, and Bax-S184K. The lowest-energy configuration of the type I simulations was used as the initial configuration for all five cases. Both with WW-IFWW and KBT-IFWW scales, no cases of any significant movement of helix α9 from the hydrophobic pocket of the Bax were registered in the case of the type II simulations for wt-Bax and Bax-S184K when the number of steps was 200,000. For the cases of the mutants Bax-S184A, Bax-S184V, and Bax-S184D, the release of helix α9 took place but without the insertion of this helix into the membrane (Supplementary Figures S1–S3). Because the data of Nechustan et al. (1999) strongly suggest the insertion of helix α9 of wt-Bax into the MOM upon the action of apoptotic stimuli and a constitutive residence in the MOM of helix α9 of mutants Bax-S184A and Bax-S184V in nonapoptotic cells, the contradiction between the experiment and the results of the simulations was hypothesized initially to be caused by an overestimated account of "lipid perturbation effect" by the KBT scale in the case when the membrane contains cardiolipin. To test this, the simulations with the use of the Radzicka–Wolfenden hydrophobicity scale (Radzicka and Wolfenden 1988), whose values are known to correspond to the solvation constituents of the KBT hydrophobicity scale values, were performed. These simulations failed also to reveal the insertion of helix α9 into the membrane. Then, in accordance with the growing evidence that the acyl tail region has some polar content, the free energies of transfer in vivo of positively charged residues, such as arginines and lysines and in particular of Lys189 and Lys190, into the MOM were suggested to be significantly below the values from any hydrophobicity scale, based on the data from water-to-alkane (cyclohexane) transfer. To test this, simulations using a hybrid KBT-LysWW-IFWW scale were undertaken. With this scale, the value of 7.4 kcal/mol for Lys from the KBT-IFWW scale was replaced with 2.71 kcal/mol from the WW-scale. The type II simulations for wt-Bax, Bax-S184A, Bax-S184V, and Bax-S184D with the use of such a hybrid scale showed profound and stable insertion of the helix α9 into the membrane for the cases Bax-S184A and Bax-S184V (see Fig. 3). Isolated cases of sufficiently deep, but unstable, insertion into the membrane took place in the case of Bax-S184D (data not shown),

while no insertion was registered in the case of wt-Bax. For this latter case, no significant displacement of helix α9 from the Bax binding groove was observed.

The strongest binding of tBid with Bax occurs at an interaction site that is distinct from the canonical binding groove of Bax

Because the experimental data for wt-Bax show the insertion of helix α9 into MOM upon the action of apoptotic stimuli (Nechustan et al. 1999), more careful analysis was undertaken. The data of Suzuki et al. (2000) suggest that hydrogen bonding between Ser184 and Asp98 prevents the release of the α9 helix from the Bax canonical binding pocket and thus this hydrogen bond should be disrupted to make α9 release feasible. It was hypothesized that a closer position of residues Ser184 and Asp98 to the negative charges of the membrane could lead to attenuation and disruption of hydrogen bonding between these residues. One way that suggests itself to induce such a translocation of these residues is through the mediation of tBid. In line with this hypothesis, the interaction of positively charged tBid with the negatively charged part of Bax could lead to the formation of a transient complex between these two proteins with the distribution of the charge of the complex favoring a displacement of the Bax-globule together with Ser184 and Asp98 closer to the membrane. To test this hypothesis, a two-stage approach was applied. At first, the 3D structure of the complex tBid–Bax was predicted with the use of the protein-protein docking computer program Hex with shape plus electrostatics correlations (Ritchie and Kemp 2000). To avoid false-negative results upon computer-automated rigid docking of flexible loops, the loops comprising residues 1–29, 39–48 of Bax, and 61–70 of tBid were eliminated prior to the docking computations. After the docking, the eliminated loops were restored and optimized within the full Bax-tBid complex with the use of program SE (Nikiforovich et al. 1979) adapted to the ECEPP2/ECEPP3 protein force-field parameterization (Dunfield et al. 1978; Némethy et al. 1983, 1992). The best score Bax-tBid complex predicted by the in-silico docking with the restored and optimized loops is shown in Fig. 4a. Within this best score structure, the interface between tBid and Bax is formed by helices H3 and H8 of tBid; Bax helices α1, α2, and α3; and the α5 helix C-terminus while the canonical binding groove of Bax is away from the interface. Of note, Asp33 of Bax and Arg84 of Bid, which were earlier shown to play a key role in the tBid–Bax interaction (Cartron et al. 2004a), lie close to each other within the predicted best score structure (shown in Fig. 4a).

The tBid–Bax interaction results in the close approach of residues Asp98-Ser184 to the membrane negative charge and release of helix α9 from the hydrophobic groove

In order to elucidate the behavior of Bax after its docking with tBid, type III simulations were applied to the protein complex tBid–Bax predicted with the use of the program Hex. The initial and lowest-energy configurations are shown in Fig. 4b and c, respectively. The simulations showed that tBid binds to the membrane by its N-terminal Arg63, turning Bax to an extent that Asp98 and Ser84 are brought into close proximity to the membrane.

Next, the type IV simulations were carried out with the use of WW-IFWW, KBT-IFWW and KBT-LysWW-IFWW scales in turn taking the lowest-energy configuration of the type III simulations as the starting point. When either the WW-IFWW scale or the KBT-IFWW scale was used, the significant exposure of helix α9 of wt-Bax from the hydrophobic groove but without helix insertion into the membrane was observed, resulting in the lowest-energy configurations, whereby Lys189 and Lys190 were located adjacent to the headgroups of the lipids (shown for the KBT-IFWW scale in Fig. 5a). The wt-Bax behavior was quite different when the simulations using the KBT-LysWW-IFWW scale were applied. In this case, a profound and stable insertion of helix α9 into the membrane was registered (Fig. 5b). As for Bax-S184K, no appreciable changes in the position of helix α9 relative to the remainder of the protein were observed.

Insertion of the α5–α6 hairpin into the membrane

To elucidate how the amphipathic hairpin α5–α6 inserts into the hydrophobic core of the MOM, Monte Carlo simulations with the initial type V configuration were carried out. No stable insertion was registered when either the WW-IFWW scale or the KBT-IFWW scale were used upon applying the type V simulations. As in the case of the α9 helix insertion, the question arises as to why we were not able to obtain the insertion of the helices α5 and α6 into the outer mitochondrial membrane, which has been reliably observed experimentally (Garcia-Saez et al. 2004; Annis et al. 2005). One way to explain the immersion of hairpin α5–α6 is to propose that the closely spaced, oppositely charged residues Glu131 and Arg134, Asp142 and Arg145 of helix 6 are salt-bridged, thus reducing their desolvation energy, and with it the free energy of their transfer into the membrane (Honig and Hubbel 1984; Wimley et al. 1996; Jayasinghe et al. 2001). To examine this hypothesis, the net transfer free energy for each ion pair was taken from the "augmented

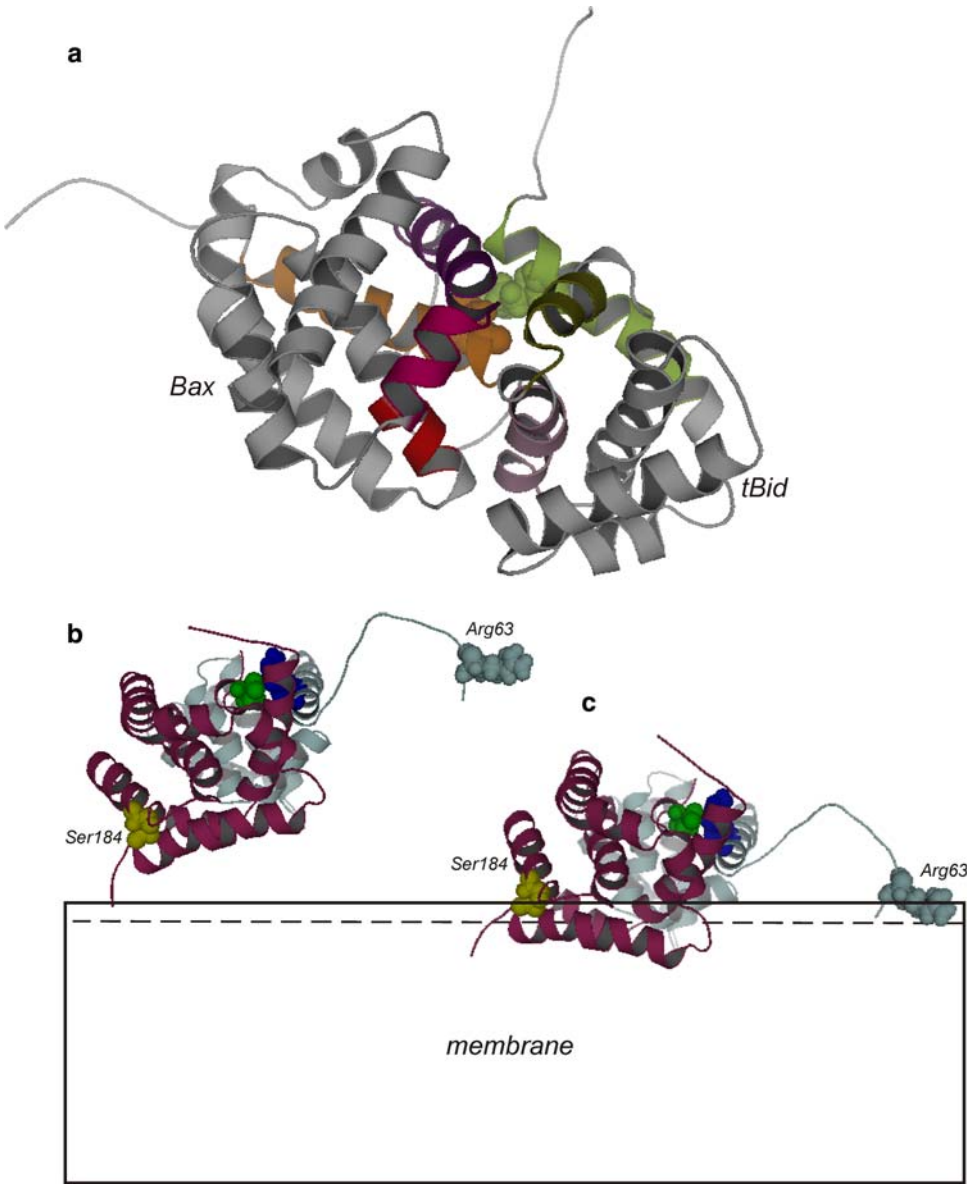

Fig. 4 **a** The conformation of the complex Bax-tBid predicted by computer docking with the use of the program Hex (Ritchie and Kemp 2000). Helices H3, H8, and H7 of tBid and α1, α2, and α3 are colored *lemon*, *deep olive*, *light pink*, *orange*, *deep purple*, and *hot pink*, respectively. The α5 C-terminus is colored *red*. Asp33 of Bax and Arg84 of Bid are shown in *spacefill*. **b** Initial configuration of type III MC simulations. **c** The lowest-energy configuration obtained by type III MC simulations for the complex Bax-tBid

WW scale" (Jayasinghe et al. 2001) when applying the WW-IFWW scale. One might expect more significant reduction in the desolvation energy if polar residues forming ion pairs are transferred from water into a hydrophobic core of the membrane ($\varepsilon_m \approx 4$) (Honig and Hubbel 1984), which is less polar than octanol ($\varepsilon_{oct} \approx 12$). Because no such data were available for transfer either to cyclohexane or to real biological membranes, the heuristic values for reduction $\Delta\Delta G_{KBT}$ of the net transfer free energy for each ion pair based on the considerations of Honig and Hubbel (Honig and Hubbel 1984) were adopted when applying the KBT-IFWW scale: $\Delta\Delta G_{KBT} = \varepsilon_{oct}/\varepsilon_{hm}\Delta\Delta G_{WW} \approx 3\Delta\Delta G_{WW}$, where $\Delta\Delta G_{WW}$ is the corresponding reduction for the WW scale calculated from the "augmented WW scale" values (Jayasinghe et al. 2001). Despite the enhanced hydrophobicity of helix α6 due to these changes, no stable insertions took place here, either, when using either the WW-IFWW or the KBT-IFWW augmented scales, although, unlike the previous consideration, isolated cases of the hairpin insertion were observed (data not shown). It was then suggested that, similarly to the case of the helix α9 insertion into the MOM, the underestimation of the polarity of the Lys119, Lys123, and Lys128 environment within the membrane hydrophobic core by KBT-scale might be responsible for failures to reproduce a stable insertion of hairpin α5–α6 into the model membrane mimicking the MOM. To test this suggestion, the

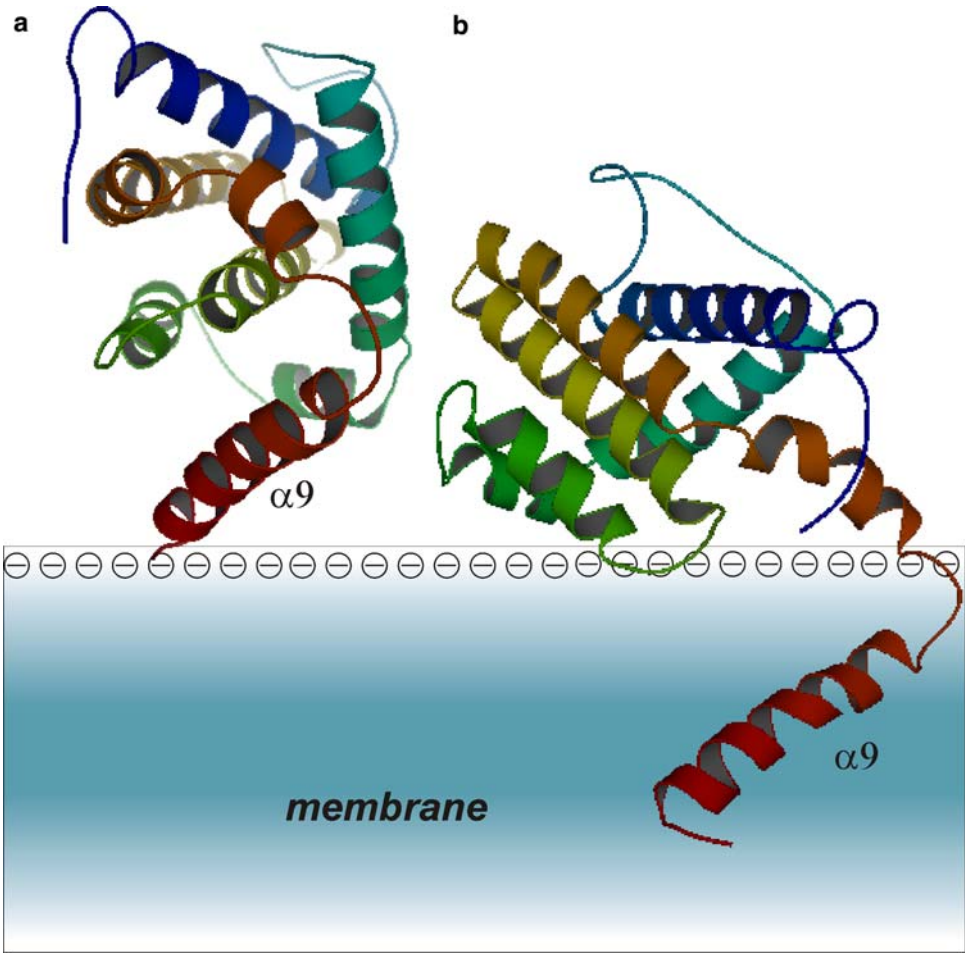

Fig. 5 The lowest-energy configuration obtained by type IV MC simulations for the complex Bax-tBid with the use of the KBT-IFWW-scale (**a**) and the KBT-LysWW-IFWW scale (**b**). For simplicity, only Bax is shown. The α9 helices are shown in *red*. The membrane hydrophobicity profile and the membrane surface charge are represented using the scheme of Fig. 2

simulations were performed with the use of the hybrid KBT-LysWW-IFWW scale. In contrast to simulations with the use of the WW-IFWW or KBT-IFWW scales, the stable insertion of the α5–α6 hairpin took place. Figure 6 shows the lowest-energy structure obtained by the Monte Carlo simulations of types V and VI. The dihedral angles and Cartesian 3D coordinates of atoms for the lowest-energy structure are shown in Supplementary Table ST1 and in Supplementary Data 4, respectively, of the electronic Supplementary Material file. When the simulations with the same scale, but without the correction for salt-bridge formation in the transfer free energy of ion pairs, were performed, the insertion of the α5–α6 hairpin into the membrane in the case of the type V simulations was not detected (data not shown). These results show that the insertion of hairpin α5–α6 into the MOM can be reproduced by the simulations upon the fulfillment of two conditions: the formation of salt-bridges between Glu131 and Arg134, Asp142 and Arg145 of the helix 6 as well as with the use of octanol-like transfer energy values for lysines.

The results obtained with different types of simulations and different hydrophobicity scales are summarized in Table 1.

Discussion

The behavior of Bax in healthy (nonapoptotic) cells

The results of the simulations show that despite the net negative charge of Bax ($\sim -4e$), the protein was not subjected to significant repulsion from the anionic membrane and possessed the lowest-energy configuration corresponding to a membrane-associated state. Mathematically, the charge of Bax (totally negative) can be decomposed into the sum of a negatively charged monopole and multipoles. At close distances to the membrane, the dipole-membrane interaction is dominant, resulting in the lowest-energy state of the system corresponding to Bax associated with the membrane by the most positively charged side of the protein (the side of the location of helix α9).

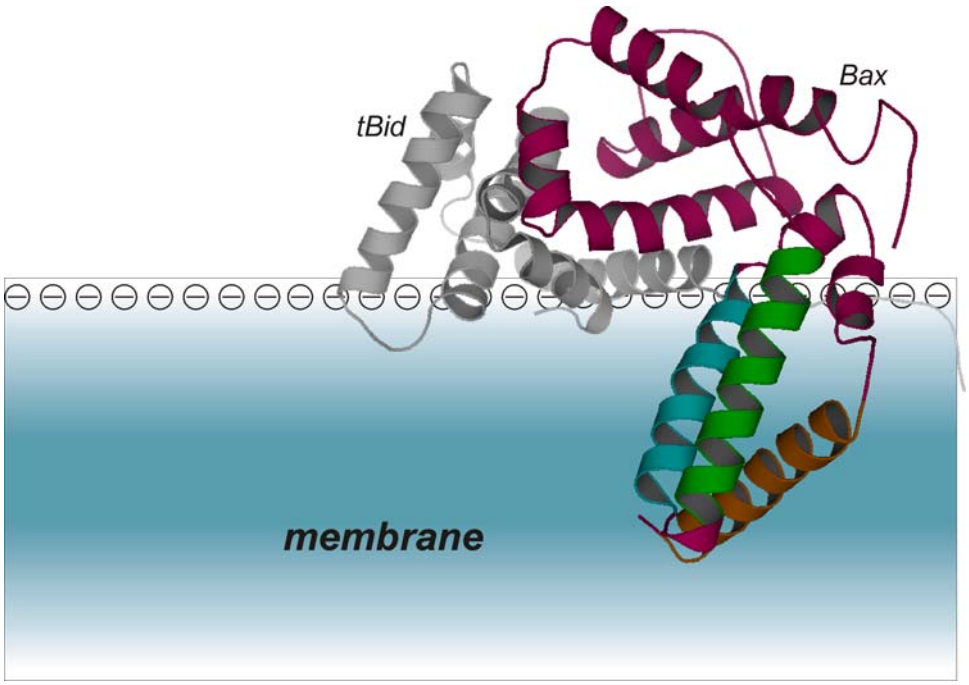

Fig. 6 A 3D structure of the complex of wt-Bax-tBid integrated into the model membrane by the Bax helices α5, α6, and α9. The lowest-energy configuration obtained by Monte Carlo type VI simulations with the use of the hybrid KBT-LysWW-IFWW scale is shown. The transfer of ion pairs was taken into account by the "augmented Wimley–White scale" (Jayasinghe et al. 2001). The lowest-energy configuration from the type V simulations was used as the starting configuration for the type VI simulations. Helices α5, α6, and α9 are colored *green*, *cyan*, and *orange*, respectively. The remainder of Bax is colored *hot pink*. tBid is depicted as *gray*. The membrane hydrophobicity profile and the membrane surface charge are represented using the scheme of Fig. 2

Kinetically, in the system with the anionic membrane and one molecule of Bax in solution, starting from an arbitrary position and orientation in the cytosol, Bax, eventually, turns to the membrane by its positive pole (formed by a cluster of positively charged residues) followed by the attraction of the protein to the membrane and weak association with it as a peripheral protein. It can be expected that if many molecules of Bax are present, an equilibrium is established between association to and dissociation from the membrane as well as between Bax molecules in solution and those in the membrane-adsorbed state. This suggests that, despite the net negative charge of Bax, a number of the protein molecules will be adsorbed to the membrane even under healthy cell conditions. This prediction is consistent with observations for a number of cell types where mitochondrially associated Bax molecules were found in healthy cells (Goping et al. 1998; Suzuki et al. 2000).

The insertion of helix α9 of Bax into the membrane

The results obtained show that while the release of helix α9 from the hydrophobic pockets of mutant proteins Bax-S184A, Bax-S184V, and Bax-S184D occurs spontaneously, that is, requiring neither the participation of other proteins nor the elevation of the net charge of these Bax mutants, we were able to reproduce such a process with wild-type form only when Bax was bound to tBid and approached, due to attraction between the positively charged tBid N-terminal fragment and negative surface charge on the membrane, in close proximity to the membrane by Asp98 and Ser184 thus making the release of helix α9 from hydrophobic groove feasible.

In accordance with this model, the N-terminal segment of tBid encompassing residues 61–78 (G61NRSSHSRL G70RIEADSES78) plays a key role in this displacement of Bax. The C-terminal sub-segment of this segment consisting of residues 61–70 was kept widely separated from the rest of the complex Bax-tBid by the N-terminal portion of this segment consisting of residues 71–78 during all runs of the type-III simulations (Fig. 4b, c) despite the fact that significant internal rotations around N–C_α and C_α–C′ bonds of Ala74 and Ser76 took place (see Table ST2 of the electronic Supplementary Material file). Such a quasi-rigidity of the sub-segment of residues 71–78 can be explained by the presence within it of a number of bulky residues that impose severe restrictions on the allowable internal motions of this portion of the tBid N-terminal segment (Flores et al. 2007), forcing it to be extended away from the rest of the complex Bax–tBid. In contrast, the

Table 1 Results obtained by the simulations of types I-VI using different hydrophobicity scales

Simulation type	Wild type or mutants used	Hydrophobicity scale used	Release of helix α9 from the Bax binding groove	Insertion of helix α9 into the membrane	Insertion of the hairpin, formed by helices α5 and α6 into the membrane
I	wt	KBT	ns	ns	ns
II	wt	KBT-IFWW, WW-IFWW	−	−	−
	S184A	KBT-IFWW, WW-IFWW	+	−	ns
	S184V	KBT-IFWW, WW-IFWW	+	−	ns
	S184D	KBT-IFWW, WW-IFWW	+	−	ns
	S184K	KBT-IFWW, WW-IFWW	−	−	ns
	wt	RW	−	−	ns
	S184A	RW	+	−	ns
	S184V	RW	+	−	ns
	S184D	RW	+	−	ns
	wt	KBT-LysWW-IFWW	−	−	−
	S184A	KBT-LysWW-IFWW	+	+	ns
	S184V	KBT-LysWW-IFWW	+	+	ns
	S184D	KBT-AspWW-IFWW	+	+/−	ns
	S184K	KBT-LysWW-IFWW	−	−	ns
IV	wt	KBT-IFWW, WW-IFWW	+	−	ns
	wt	KBT-LysWW-IFWW	+	+	ns
	S184K	KBT-LysWW-IFWW	−	−	ns
V	wt	KBT-IFWW, WW-IFWW	+	+	−
V	wt	KBT-LysWW-IFWW without the correction for salt-bridges formation	+	+	−
V, VI	wt	KBT-LysWW-IFWW with the correction for salt-bridges formation	+	+	+

ns Not simulated, *RW* Radzicka–Wolfenden scale (Radzicka and Wolfenden 1988)

presence within the N-terminal sub-segment (residues 61–70) of one glycine (Gly70) and of a considerable number of residues with small sizes of side chains, among which there are two sequential pairs of residues Leu69, Gly70 and Ser64, Ser65, suggests that this portion is far more flexible. In accordance with this hypothetical scheme, whereby the N-terminal segment of tBid (residues 61–78) consists of a rather flexible N-terminal sub-segment (residues 61–70) and a rather rigid C-terminal sub-segment (residues 71–78), rigidly attached to the rest of the complex Bax-tBid, the latter sub-segment of the N-terminal segment of tBid (encompassing residues 71–78) keeps the most flexible portion (consisting of residues 61–70) separated from the rest of the complex state, while the most flexible one acts as a "rope" dragging the rigid rest of the complex closer to the membrane, resulting finally in the lowest-energy structure shown in Fig. 4c.

When either WW-IFWW or KBT-IFWW hydrophobicity scales were applied to wt-Bax with a disrupted hydrogen bond between Ser184 and Asp98 or to the mutants Bax-Ser184Ala and Bax-Ser184Val without such a bond, no cases of insertion of helix α9 into the membrane were registered. Per residue analysis showed that this was caused by the high free-energy cost of the transfer of charged Lys189 and Lys190 from the polar membrane interface environment into the hydrophobic environment of the membrane core (data not shown). However, when KBT-LysWW-IFWW scale was used, the stable insertion of helix α9 into the membrane was revealed in the cases of wt-Bax and mutants Bax-Ser184Ala and Bax-Ser184Val, but not in the case of Bax-Ser184Asp.

The disruption of hydrogen bonding between Ser184 and Asp98 of wt-Bax is a key event in Bax integration into the MOM. The simulations showed that the increase in free energy due to the separation of the hydroxyl group of Ser184 from the carboxylate group of Asp98 is initially compensated for by the decrease of the electrostatic energy due to interaction of Lys 189 and Lys190 with the surface negative charge (corresponding to the plane of lipid headgroups) with an ensuing additional free-energy gain

due to immersion of hydrophobic residues of helix α9 into a nonpolar environment. The latter effect was taken into account both by the electrostatic term describing the repulsion of Asp98 side chain from the membrane and by the hybrid KBT-LysWW-IFWW scale, whereby Ser184 prefers to be located in the headgroup region, while the preferred position of the hydrophobic residues of helix α9 is within the hydrophobic core. A significant reduction in the free-energy barrier for such a transition of helix α9 from a potential well, caused by interaction of Ser184 with Asp98, to another potential well, caused by interaction of C-terminal lysines with the surface negative charges, is achieved by the approach of the hydrogen-bonded pair Ser184-Asp98 close to the membrane surface charges.

The insertion of the α9 helix containing charged lysines into the MOM seems to have much in common with the transfer through the lipid phase of the highly charged S4 helix of the KvAP voltage-dependent potassium channel (Jiang et al. 2003; Hessa et al. 2005). Molecular dynamics studies of the S4 helix movement through a lipid bilayer showed the possibility of two not necessarily mutually exclusive mechanisms of compensation for high free-energy costs of charge transfer through the lipid phase: by either interaction with water or with lipid headgroups (Freites et al. 2005; Sands and Sansom 2007; Bond and Sansom 2007). Recently, a lipid phosphate-mediated arginine insertion into lipid membranes has been revealed by solid-state NMR (Tang et al. 2007). These data suggest that cationic residues can, at least in some cases, drag anionic phosphate groups along as they insert into the hydrophobic part of the membrane, thus creating a polarity-favorable environment for the charged side chains of these residues within the hydrocarbon core of the bilayer. Taken together, our results and those of other authors argue in favor of the mechanism of the Bax anchoring by helix α9, whereby the formation of complexes of Lys189 and Lys190 either with water molecules or with lipid anionic phosphate groups facilitates insertion of the helix into the membrane.

When Ser184 was replaced with Lys, the release of helix α9 from the Bax hydrophobic pocket was abolished. In this case, the formation of a salt bridge between Lys184 and Asp98 took place, which hindered dissociation of the C-terminal helix from the hydrophobic pocket (data not shown). Though the replacement of Ser184 with Asp promoted dissociation of helix α9 from the hydrophobic pocket, no insertions into the membrane were registered in this case either. This result can be explained by a large free-energy penalty for the transfer of the aspartate into the hydrocarbon core of the membrane as well as by repulsion of the negatively charged aspartate from the negatively charged plane in the membrane surface layer. However, when the KBT value for Asp184 was replaced by that from the WW scale, isolated cases of sufficiently deep insertion were observed (data not shown). The data of Nechustan et al. (1999) showed the stable integration of the mutants Bax-Ser184Ala and Bax-Ser184Val into the MOM, but the absence of such integration for the mutant Bax-Ser184Asp. In general, our results suggest that the addition of a third polar residue to helix α9 changes the sign of the balance among hydrophobic, electrostatic, and elastic interactions of Bax with the membrane thus making the stable insertion of the helix into the hydrophobic core of the MOM infeasible. These results showed that while the α9-helix insertion into the membrane in the case of wild-type Bax and the mutants Bax-Ser184Val and Bax-Ser184Ala is energetically favorable, the reverse is true when Ser184 is substituted for a more polar residue. This suggests that a hydrophobicity effect overcomes the net effect of the electrostatic and elastic repulsion in the former case, while exactly the opposite net effect takes place in the latter case.

It may be suggested that a close approach of the hydrogen-bonded pair Asp98-Ser184 to anionic phosphate headgroups, similar to that caused by tBid, can also be achieved by making the charge of Bax more positive, as for instance, by lowering pH. Bax activation and apoptosis in several cell types in response to pH drop seem to be in agreement with this suggestion [see Matsuyama et al. (2000), Cartron et al. (2004b) and references therein]. These data were initially interpreted as if the changes in pH would lead directly to changes in the solution conformation of Bax thus favoring Bax integration into the MOM and its permeabilization (Khaled et al. 1999). However, when Bax is in solution, such conformational changes were demonstrated by the NMR data to be absent (Suzuki et al. 2000), thus ruling out the possibility that a drop in pH could trigger Bax activation through effects on conformational rearrangements in solution. Collectively, the latter conclusion and the considerations above suggest a different interpretation, whereby the increase in proton concentration can increase the Bax net charge by protonation of a number of Bax titratable groups, resulting in stronger attraction of Bax to the MOM and displacement of the Bax pair of residues Asp98-Ser184 close to the membrane followed by hydrogen-bond disruption, release of helix α9, and its insertion into the MOM.

Insertion of the hairpin formed by helices α5 and α6 into the membrane

The membrane insertion of the Bax TM domain and the integration of helices 5 and 6 into the MOM lipid bilayer are thought to contribute to pore formation, which in turn might allow the release of intermembrane space proteins such as cytochrome *c*. This concept is based in part on the structural similarities between Bax and the pore-forming domains of diphtheria toxin and colicins, an idea that has

contributed to the notion that Bax oligomerization occurs prior to or concomitant with the insertion of helices 5 and 6 into the MOM bilayer. This is in contrast, however, to the findings of Annis et al. (2005), who argued that, unlike some pore-forming proteins, Bax forms membrane-integrated monomers in which all three helices, α5, α6, and α9, are inserted into the bilayer prior to Bax oligomerization. The simulations showed that, when starting from the structure with the inserted helix α9 and with the remainder of the protein either on the membrane surface or exposed to the solvent (type V simulations), wt-Bax can adopt the transbilayer orientation of the hairpin formed by helices α5 and α6 spontaneously, but only upon the fulfillment of two conditions. These are the formation of ion pairs by the side chains of the oppositely charged residues of the α6 helix and an octanol-like-polarity environment around positively charged residues of helix α5 within the bilayer interior. As to the former assumption, its use may be thought of as justified in view of a number of theoretical and experimental results (Wimley et al. 1996; Chin and Heijne 2000; Jayasinghe et al. 2001) that reveal the significant thermodynamic stabilization of charged residues within a hydrophobic environment due to formation of salt-bridges. As to the second condition, it is based on the assumption that the octanol-like-polarity environment around lysine side chains within the hydrocarbon core of the membrane is achieved by the complexation of the side chains either with water molecules, which were shown to accompany basic or acidic residues buried in the hydrocarbon core of the bilayer (Dwyer et al. 2000), or with lipid phosphate headgroups accompanying, supposedly, lysine side chains within the membrane. Recently, similar complexation of positively charged residues with lipid phosphates resulting in a phosphate-mediated insertion of these residues into lipid membranes has been revealed by solid-state NMR (Tang et al. 2007). If this is the case when Bax inserts into the MOM, it may be suggested that Lys119 and Lys123 perform the function of carriers of structural materials for the construction of toroidal pores. Several years ago, Nouraini et al. (2000) performed a comprehensive analysis of the role of charged residues from hairpin α5–α6 in the insertion and killing activity of Bax. They showed that the substitution of Lys119 and Lys123 by alanines [the mutagenic alterations B of Nouraini et al. (2000)], or the same substitutions of Lys119, Lys123, Asp142, Arg145, and Glu146 [the mutagenic alterations C (Nouraini et al. 2000)] favored the expression of a gain-of-function phenotype when expressed in mammalian cells, while the mutagenic alteration F (Arg109Ala, Lys119Ala, Lys123Ala, Lys128Ala, Arg134Ala, Asp142Ala, Arg145Ala, and Glu146Ala) resulted in a loss of cytotoxicity in yeast. In view of our results, the data of Nouraini et al. can be interpreted as that the mutagenic alterations B and C impart the enhanced hydrophobicity to helix α5, while the mutagenic substitutions F disturb ion pairs in helix α6. Collectively, the results of our simulations argue both in favor of the formation of ion pairs when the isolated α6 helix inserts into the membrane and in favor of the creation of suitable polarity conditions for the insertion of the lysines of helix α5.

Recently, Garcia-Saez et al. (2004) have demonstrated the spontaneous insertion of the α5–α6 helical hairpin into microsomal membranes. Our results and the considerations above explain these data by the significant reduction in the free-energy barrier for the insertion of helices α5 and α6 into the membrane due to the formation of ion pairs between closely spaced, oppositely charged residues Glu131 and Arg134, Asp142 and Arg145 of helix 6 as well as due to the complexation of the side chains of Lys119 and Lys123 either with water molecules or with lipid phosphates accompanying, supposedly, lysine side chains within the membrane.

The model of Bax activation by tBid

Even using the hybrid KBT-LysWW-IFWW scale, the release of the wt-Bax helix α9 from the binding pocket on the surface of Bax and subsequent insertion of the helix into the model membrane mimicking the MOM became feasible only in the case of a close approach of residues Ser184 and Asp98 to the plane of negative charge in the membrane surface layer. Our results show that such an energy-driven process, which favors the approach of Bax to negative electrical charges in the membrane surface layer, can occur due to the association of Bax with tBid.

Bid has long been suggested as a likely candidate for the protein responsible for driving the Bax integration (insertion) into the mitochondrial membrane (Desagher et al. 1999; Eskes et al. 2000; Kuwana et al. 2002; Terrones et al. 2004). The most popular model suggested that the tBid BH3 domain may trigger the exposure of the helix α9 by displacing it from the binding groove on the Bax surface (Roucou et al. 2002). However, the results of Suzuki et al. (2000) showed that binding of the BH3 domain of another Bcl-2 family member would not be enough to disrupt the interactions between the C-terminal tail of Bax and its hydrophobic pocket. At first glance, this conclusion seems contrary to the experimental evidence that in the case of pure synthetic liposomes tBid alone is sufficient to activate Bax (Kuwana et al. 2002; Terrones et al. 2004). However, both results can be reconciled if one assumes a mechanism of Bax activation by tBid, different from a direct disruption of the hydrogen bond between Ser184 and Asp98 by the BH3 domain of tBid. The results of our simulations suggest that the formation of a complex between Bax and positively charged tBid can significantly reduce, due to

interaction between the positive charges of tBid and the negative charges of the membrane, the energy barrier that prevents the approach of Ser184 and Asp98 to the anionic headgroups of membrane lipids, thus leading to attenuation and disruption of the hydrogen bond between these two residues. In accordance with this interpretation of Bax activation, tBid is required primarily for a close approach of residues Ser184 and Asp98 to the negative charges of the membrane.

Quite recently, simultaneous measurements by fluorescence techniques of tBid and Bax behavior in the course of liposome membrane permeabilization were reported (Lovell et al. 2008). These measurements suggested an ordered series of steps occurring during this process: (1) rapid tBid binding to the membrane where (2) tBid interacts with Bax causing (3) Bax insertion into membranes and (4) oligomerization, culminating in (5) membrane permeabilization. These data can be reconciled with our results if the data of Lovell et al. (2008) are interpreted somewhat differently than the authors do. It may be suggested that rapidly moving tBid molecules bind not only to the membrane, but also to the Bax molecules that were weakly adsorbed to the membrane surface and that tBid molecules that bind to membrane-adsorbed Bax molecules are precisely those that cause Bax integration into the membrane by the above-described mechanisms. Figure 7 shows a model for Bax membrane targeting and insertion based on the results obtained and the above considerations. This model, although incomplete, provides a basic mechanistic framework that can be expanded and refined as appropriate, based on future studies.

Our results seem at the first glance to be in conflict with the recent data of Kuwana et al. (2005) and Walensky et al. (2006), which showed the activation of recombinant Bax by Bim and Bid BH3 peptides. Over an extended period of time, these data have been interpreted as a displacement of Bax α9 helix from the Bax hydrophobic groove by the direct interaction with the BH3 peptides. However, recent NMR analysis of the structure of Bim-SAHB-Bax complex (Gavathiotis et al. 2008) showed that Bim BH3-peptide binds to Bax near its N-terminus, rather than near its C-terminus, thus casting doubt on the notion that the α9 helix disengagement from Bax binding groove occurs due to its direct interaction with such activators as Bim or Bid

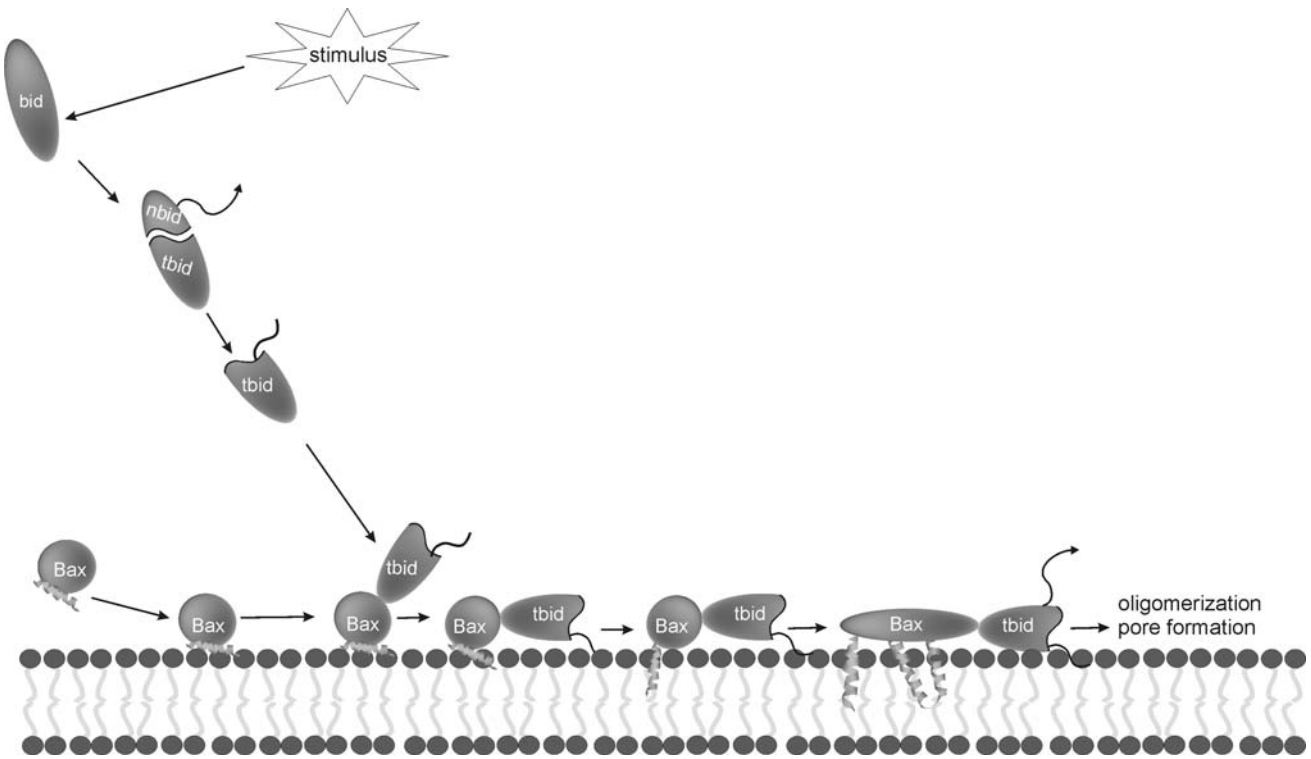

Fig. 7 The putative model of the activation of Bax by tBid upon the action of an apoptotic stimulus. In accordance with this model, in response to stimuli of the extrinsic, death receptor, pathway, Bid is proteolytically cleaved by caspase-8. The molecules of caspase-8-cleaved Bid, tBid, rapidly move, due to electrostatic attraction by MOM surface charge, in the direction of the mitochondrial outer membrane, where they bind either to the MOM or to Bax molecules adsorbed on the MOM surface. Those bound to Bax molecules displace them in such a way that the hydrogen-bonded residues Ser184 and Asp98 are brought into close proximity with the headgroup region where the free-energy barrier for the hydrogen-bond disruption is low. The disruption of the hydrogen bond leads first to insertion of the helix α9 and then to insertion of the hairpin α5–α6 into the MOM followed by oligomerization and pore formation

BH3 peptides, or full-chain tBid. The authors proposed the mechanism of Bax activation by Bim BH3 peptide in accordance with which the binding of BH3 peptide at the groove formed by helices α1 and α6 leads to Bax conformational rearrangements resulting in disengagement of helix α9 from the Bax canonical binding groove. The analysis of the protein docking between tBid and Bax predicted by the program Hex showed that tBid engages Bax at a location close to that for Bim BH3 peptide established by Gavathiotis et al. (2008) but nonetheless distinct from it. If this is the case, it can be concluded that the mechanisms of Bax activation by BH3 peptides and by tBid are different. Of note, data have been reported showing that Bax targeting to mitochondria occurs via both tail anchor-dependent and -independent, preceded by oligomerization, mechanisms (Valentijn et al. 2008). On account of these data and new data on binding Bim BH3 peptide with Bax (Gavathiotis et al. 2008), the mechanism of Bax activation by Bim BH3 peptide via the release of helix α9 seems unlikely, and therefore, tail anchor-independent mechanism of Bax integration into the MOM via a preliminary oligomerization can be hypothesized in this case.

While it may be speculated that the Bax transition from its folded state in solution to a membrane-integrated partly unfolded state is thermodynamically favored, it cannot be excluded that carrying out this process kinetically would require overcoming a significant energy barrier. This suggests that while two stages of Bax integration into the membrane, those of the membrane anchoring by helix α9 and the hairpin α5–α6 insertion into the membrane, have prerequisites to be performed either spontaneously or in combination with tBid, it cannot be excluded that, for the transition from the state with α9 inserted to that with α5, α6, and α9 inserted or further to the oligomerization-competent state, the participation of other protein(s) is necessary. The finding that active Bax in the presence of tBid can permeabilize synthetic cardiolipin-containing liposomes devoid of any other proteins (Kuwana et al. 2002), as well as the recent data of Sanjuan Szklarz et al. (2007), seem, at first glance, to argue against this hypothesis. However, other data indicate that the participation of TOM is required for tBid/Bax-induced MOM permeabilization and cytochrome *c* release (Ott et al. 2007).

A principal feature of the model membrane used in our simulations was the presence of a surface negative charge taking implicitly into account the charge of MOM anionic lipids, supposedly of cardiolipins of the MOM contact sites, because cardiolipins or their negatively charged derivatives were shown to be important for the activities of some members of the Bcl-2 family (Gonzalvez and Gottlieb 2007). However, while the role of cardiolipin in membrane permeabilization by tBid and Bax in vitro has been well documented (Kuwana et al. 2002), its in vivo relevance in MOM permeabilization still remains controversial (Polcic et al. 2005). Quite recently, based on a series of studies with liposomes containing native MOM material, Kuwana and coworkers concluded (Schafer et al. 2009) that the role of cardiolipins in the permeabilization of synthetic cardiolipin-containing membranes by tBid and Bax (Kuwana et al. 2002) is played in physiological MOM permeabilization by some protein(s) from the MOM and that this protein is a receptor for tBid. If this is the case, the scenario similar to that proposed by our model can be hypothesized but with negative charges provided by these proteins rather than by cardiolipins.

One prediction emerging from our model can be considered as one of its critical tests. It concerns N-terminus arginines of tBid (Arg63 and Arg68), which in accordance with our model must play a key role in Bax activation and apoptosis. To the best of our knowledge, mutagenesis studies with these tBid residues have not yet been performed and are worthy of carrying out.

Concluding remarks

Several conclusions of this work are based on failures to reproduce the insertion of helices α9, α5, and α6 into the membrane during specific types of the simulations. However, membrane insertion of polar protein domains involves, in a number of cases, crossing a large free-energy barrier due to the excessive free-energy penalty associated with charge transfer from the aqueous phase into the hydrophobic core of the lipid bilayer. If the free-energy barrier is high enough, overcoming this barrier may require a sufficiently large free-energy fluctuation the likelihood of which during MC simulations depends strongly both on the barrier height and on the number of iterations. This leaves room for cases when the number of MC steps may be insufficient to reproduce the actual behavior of the protein. However, at such stages of Bax integration into the MOM as the insertion of helices α9, α5, and α6 when Bax is already bound to the membrane, both direct and indirect experimental data suggest that these processes are fast enough and therefore the free-energy barrier for the insertion is not too high.

The results presented in this paper have been made possible due to a reduction of the configurational search space by the use of experimental, biochemical, and biophysical data, physical and evolutionary considerations as well as of the implicit membrane model. Because the direct experimental determination of the structure of Bax and its complexes in the membrane environment is likely to be many years away, the application of such an integrated approach that combines a computational analysis

using an implicit membrane model with experimental analyses seems to be almost the only way at present to achieve physiologically meaningful atom-resolution models. Of course, being *an effective medium* approximation, an implicit model of the bilayer only approximately mimics the molecular properties of lipids. However, by using empirical partitioning and transfer data, and fitting the bilayer functions to experimental results, many of the molecular properties of lipids are accounted for implicitly within the parameters of the model. Due to such a combined approach, several stages of integration of Bax into the model membrane mimicking implicitly the main physical features of the MOM were described with a level of detail that is not accessible to experiment alone.

The results obtained have culminated in a novel model of Bax activation by tBid upon apoptosis. The model explains the structural basis for a number of important stages of the MOM permeabilization, many of which previously seemed obscure or contradictory. Though certain simplifications were used in the simulations, the results obtained allowed us to successfully reproduce and interpret existing data. The model of Bax activation and the structural data presented in this paper provide experimentalists with testable hypotheses as to Bax and tBid behavior during apoptotic process and also as to the plausible 3D structures of Bax in a number of its intermediate functionally important MOM-bound states preceding the oligomerization state. Because membrane proteins are notoriously difficult to manipulate experimentally, predictions such as these that suggest potential structures and their rearrangements could greatly aid our understanding of the interactions between proteins and membranes and can direct and complement experimental research.

Acknowledgments The authors thank Prof. Gregory Nikiforovich (Washington University School of Medicine, St. Louis, Missouri) and Dr Andrew Riley (Bath University, UK) for reading the early version of the manuscript and their insightful comments. This work was supported by Basic Research Foundation of Belarus (Grant B07-234) and by the Program "Bioengineering and Biosecurity" of Republic of Belarus (Grant P-16).

References

Annis MG, Soucie EL, Dlugosz PJ, Cruz-Aguado JA, Penn LZ, Leber B, Andrews DW (2005) Bax forms multispanning monomers to permeabilize membranes during apoptosis. EMBO J 24:2096–2103. doi:10.1038/sj.emboj.7600675

Antonsson B, Montessuit S, Sanchez B, Martinou J-C (2001) Bax is present as a high molecular weight oligomer/complex in the mitochondrial membrane of apoptotic cells. J Biol Chem 276:11615–11623. doi:10.1074/jbc.M010810200

Ardail D, Privat JP, Egret-Charlier M, Levrat C, Lerme F, Louisot P (1990) Mitochondrial contact sites lipid composition and dynamics. J Biol Chem 265:18797–18802

Ash WL, Zlomislic MR, Oloo EQ, Tieleman DP (2004) Computer simulations of membrane proteins. Biochim Biophys Acta 1666:158–189. doi:10.1016/j.bbamem.2004.04.012

Baumgaertner A (1996) Insertion and hairpin formation of membrane proteins: a Monte Carlo study. Biophys J 71:1248–1255. doi:10.1016/S0006-3495(96)79324-4

Bond PJ, Sansom MS (2006) Insertion and assembly of membrane protein via simulation. J Am Chem Soc 128:2697–2704. doi:10.1021/ja0569104

Bond PJ, Sansom MS (2007) Bilayer deformation by the Kv channel voltage sensor domain revealed by self-assembly simulations. Proc Natl Acad Sci USA 104:2631–2636. doi:10.1073/pnas.0606822104

Bond PJ, Holyoake J, Ivetac A, Khalid S, Sansom MS (2007) Coarse-grained molecular dynamics simulations of membrane proteins and peptides. J Struct Biol 157:593–605. doi:10.1016/j.jsb.2006.10.004

Capano M, Crompton M (2002) Biphasic translocation of Bax to mitochondria. Biochem J 367:169–178. doi:10.1042/BJ20020805

Cartron PF, Oliver L, Mayat E, Meflah K, Vallette FM (2004a) Impact of pH on Bax conformation, oligomerization and mitochondrial integration. FEBS Lett 578:41–46. doi:10.1016/j.febslet.2004.10.080

Cartron PF, Gallenne T, Bougras G, Gautier F, Manero F, Vusio P, Meflah K, Vallette FM, Juin P (2004b) The first alpha helix of Bax plays a necessary role in its ligand-induced activation by the BH3-only proteins Bid and PUMA. Mol Cell 16:807–818. doi:10.1016/j.molcel.2004.10.028

Chin C-N, Heijne G (2000) Charge pair interactions in a model transmembrane helix in the ER membrane. J Mol Biol 303:1–5. doi:10.1006/jmbi.2000.4122

Danial NN, Korsmeyer SJ (2004) Cell death: critical control points. Cell 116:205–219. doi:10.1016/S0092-8674(04)00046-7

Desagher S, Osen-Sand A, Nichols A, Esker R, Montessuit S, Lauper S, Maundrell K, Antonsson B, Martinou J-C (1999) Bid-induced conformational change of Bax is responsible for mitochondrial cytochrome c release during apoptosis. J Cell Biol 144:891–901. doi:10.1083/jcb.144.5.891

Dunfield LG, Burgess AW, Scheraga HA (1978) Energy parameters in polypeptides. 8. Empirical potential energy algorithm for the conformational analysis of large molecules. J Phys Chem 82:2609–2616. doi:10.1021/j100513a014

Dwyer JJ, Gittis AG, Karp DA, Lattman EE, Spencer DS, Stites WE, Garcia-Moreno EB (2000) High apparent dielectric constants in the interior of a protein reflect water penetration. Biophys J 79:1610–1620. doi:10.1016/S0006-3495(00)76411-3

Eskes R, Desagher S, Antonsson B, Martinou J-C (2000) Bid induces the oligomerization and insertion of Bax into the outer mitochondrial membrane. Mol Cell Biol 20:929–935. doi:10.1128/MCB.20.3.929-935.2000

Flores SC, Lu LJ, Yang J, Carriero N, Gerstein MB (2007) Hinge Atlas: relating protein sequence to sites of structural flexibility. BMC Bioinformatics 8:167. doi:10.1186/1471-2105-8-167

Fraczkiewicz R, Braun W (1998) Exact and efficient analytical calculation of the accessible surface areas and their gradients for macromolecules. J Comput Chem 19:319–333. doi:10.1002/(SICI)1096-987X(199802)19:3<319::AID-JCC6>3.0.CO;2-W

Franzin CM, Choi J, Zhai D, Reed JC, Marassi FM (2004) Structural studies of apoptosis and ion transport regulatory proteins in membranes. Magn Reson Chem 42:172–179. doi:10.1002/mrc.1322

Freites JA, Tobias DJ, von Heijne G, White SH (2005) Interface connections of a transmembrane voltage sensor. Proc Natl Acad Sci USA 102:15059–15064. doi:10.1073/pnas.0507618102

Garcia-Saez AJ, Mingarro I, Perez-Paya E, Salgado J (2004) Membrane-insertion fragments of Bcl-XL, Bax and Bid. Biochemistry 43:10930–10943. doi:10.1021/bi036044c

Gavathiotis E, Suzuki M, Davis ML, Pitter K, Bird GH, Katz SG, Tu H-C, Kim H, Cheng EH-Y, Tjandra N, Walensky LD (2008) Bax activation is initiated at a novel interaction site. Nature 455:1076–1081. doi:10.1038/nature07396

Gonzalvez F, Gottlieb E (2007) Cardiolipin: setting the beat of apoptosis. Apoptosis 12:877–885. doi:10.1007/s10495-007-0718-8

Goping IS, Gross A, Lavoie JN, Nguen M, Jemmerson R, Roth K, Korsemeyer SJ, Shore GC (1998) Regulated targeting of BAX to mitochondria. J Cell Biol 143:207–215. doi:10.1083/jcb.143.1.207

Heimlich G, McKinnon AD, Bernardo K, Brdiczka D, Reed JC, Kain R, Kronke M, Jurgmeister JM (2004) Bax-induced cytochrome c release from mitochondria depends on a-helices 5 and -6. Biochem J 378:247–255. doi:10.1042/BJ20031152

Hessa T, White SH, von Heijne G (2005) Membrane insertion of a potassium-channel voltage sensor. Science 307:1427. doi:10.1126/science.1109176

Honig BH, Hubbel WL (1984) Stability of "salt bridges" in membrane proteins. Proc Natl Acad Sci USA 81:5412–5416. doi:10.1073/pnas.81.17.5412

Jayasinghe S, Hristova K, White SH (2001) Energetics, stability, and prediction of transmembrane helices. J Mol Biol 312:927–934. doi:10.1006/jmbi.2001.5008

Jiang Y, Rutta V, Chen JY, Lee A, MacKinnon R (2003) The principles of gating charge movement in a voltage-dependent K+ channel. Nature 423:42–48. doi:10.1038/nature01581

Kessel A, Ben-Tal N (2002) Free energy determinants of peptide association with lipid bilayers in peptide–lipid interactions. In: Simons SA, McIntosh TJ (eds) Current topics in membranes, vol 52. Academic Press, San Diego, pp 205–253

Kessel A, Shental-Bechor D, Haliloglu T, Ben-Tal N (2003) Interaction of hydrophobic peptides with lipid bilayers: Monte Carlo simulations with M2d. Biophys J 85:3431–3444. doi:10.1016/S0006-3495(03)74765-1

Khaled AR, Kim K, Hofmeister R, Muegge K, Durum SK (1999) Withdrawal of IL-7 induces Bax translocation from cytosol to mitochondria through a rise in intracellular pH. Proc Natl Acad Sci USA 96:14476–14481. doi:10.1073/pnas.96.25.14476

Kroemer G, Galluzzi L, Brenner C (2007) Mitochondrial membrane permeabilization in cell death. Physiol Rev 87:99–163. doi:10.1152/physrev.00013.2006

Kuwana T, Mackey MR, Perkins G, Ellisman MH, Latterich M, Schneiter R, Green DR, Newmeyer DD (2002) Bid, Bax, and lipids cooperate to form supramolecular openings in the outer mitochondrial membranes. Cell 111:331–342. doi:10.1016/S0092-8674(02)01036-X

Kuwana T, Bouchier-Hayes L, Chipuk JE, Bonzon C, Sullivan BA, Green DR, Newmeyer DD (2005) BH3 domains of BH3-only proteins differentially regulate Bax-mediated mitochondrial. Mol Cell 17:525–535. doi:10.1016/j.molcel.2005.02.003

Leber B, Lin J, Andrews DW (2007) Embedded together: the life and death consequences of interaction of the Bcl-2 with membranes. Apoptosis 12:897–911. doi:10.1007/s10495-007-0746-4

Linseman DA, Butts BD, Precht TA, Phelps RA, Le SS, Laessig TA, Bouchard JR, Florez-McClure ML, Heidenreich KA (2004) Glycogen synthase kinase-3beta phosphorylates Bax and promotes its mitochondrial localization during neuronal apoptosis. J Neurosci 24:9993–10002. doi:10.1523/JNEUROSCI.2057-04.2004

Lovell JF, Billen LP, Bindner S, Shamas-Din A, Fradin C, Leber B, Andrews DA (2008) Membrane binding by tBid initiates an ordered series of events culminating in membrane permeabilization by Bax. Cell 135:1074–1084. doi:10.1016/j.cell.2008.11.010

Lutter M, Fang M, Luo X, Nishijima M, Xie X, Wang X (2000) Cardiolipin provides specificity for targetting of tBid to mitochondria. Nat Cell Biol 2:754–761. doi:10.1038/35036395

MacCallum JL, Bennet WFD, Tieleman DP (2007) Partitioning of amino acid side chains into lipid bilayers: results from computer simulations and comparison to experiment. J Gen Physiol 129:371–377. doi:10.1085/jgp.200709745

Matsuyama S, Llopis J, Deveraux OL, Tsien RY, Reed JC (2000) Changes in intramitochondrial and cytosolic pH: early events that modulate caspase activation during apoptosis. Nat Cell Biol 2:318–325. doi:10.1038/35014006

Nechustan A, Smith CL, Hsu YT, Youle RJ (1999) Conformation of the BAX C-terminus regulates subcellular location and cell death. EMBO J 18:2330–2341. doi:10.1093/emboj/18.9.2330

Némethy G, Pottle MS, Scheraga HA (1983) Energy parameters in polypeptides 9. Updating of geometrical parameters, nonbonded interactions, and hydrogen bond interactions for the naturally occurring amino acids. J Phys Chem 87:1883–1887. doi:10.1021/j100234a011

Némethy G, Gibson KD, Palmer KA, Yoon CN, Paterlini G, Zagari A, Rumsey S, Scheraga HA (1992) Energy parameters in polypeptides 10. Improved geometrical parameters and nonbonded interactions for use in ECEPP/3 algorithm with application to proline-containing peptides. J Phys Chem 96:6472–6484. doi:10.1021/j100194a068

Nikiforovich GV, Leonova VJ, Galaktionov SG, Chipens GI (1979) Theoretical conformational analysis of oxytocin molecule. Int J Pept Protein Res 13:363–373

Nouraini S, Six E, Matsuyama S, Krajevski S, Reed J (2000) The putative pore forming domain of Bax regulates mitochondrial localization and interaction with Bcl-XL. Mol Cell Biol 20:1604–1615. doi:10.1128/MCB.20.5.1604-1615.2000

Oh KJ, Barbutto S, Pitter K, Morash J, Walensky LD, Korsemeyer SJ (2006) A membrane-targeted BID BCL-2 homology 3 peptide is sufficient for high potency activation of BAX in vitro. J Biol Chem 281:36999–37008. doi:10.1074/jbc.M602341200

Oliver L, Priault M, Tremblais K, LeCabellec M, Meflah K, Manon S, Vallette FM (2000) The substitution of the C-terminus of Bax by that of bcl-xL does not affect its subcellular localization but abrogates its pro-apoptotic properties. FEBS Lett 487:161–165. doi:10.1016/S0014-5793(00)02330-9

Ott M, Nornberg E, Walter KM, Schreiner P, Kemper C, Rapoport D, Zhivotovsky B, Orrenius S (2007) The mitochondrial TOM complex is required for tBid/Bax-induced cytochrome c release. J Biol Chem 282:27633–27639. doi:10.1074/jbc.M703155200

Parker MW, Feil SC (2005) Pore-forming protein toxins from structure to function. Prog Biophys Mol Biol 88:91–142. doi:10.1016/j.pbiomolbio.2004.01.009

Peitzsch RM, Eisenberg M, Sharp KA, McLaughlin S (1995) Calculations of the electrostatic potential adjacent to model phospholipid bilayers. Biophys J 68:729–738. doi:10.1016/S0006-3495(95)80253-5

Polcic P, Su X, Fowlkes J, Blashy-Dyson E, Dowhan W, Forte M (2005) Cardiolipin and phosphatidylglycerol are not required for the in vivo action of Bcl-2 family proteins. Cell Death Differ 12:310–312. doi:10.1038/sj.cdd.4401566

Radzicka A, Wolfenden R (1988) Comparing the polarities of the amino acids: side-chain distribution coefficients between the vapor phase, cyclohexane, *l*-octanol, and neutral aqueous solution. Biochemistry 27:1664–1670. doi:10.1021/bi00405a042

Ritchie DW, Kemp GJL (2000) Protein docking using spherical polar Fourier correlations. Proteins 39:178–194. doi:10.1002/(SICI)1097-0134(20000501)39:2<178::AID-PROT8>3.0.CO;2-6

Roucou X, Rostovtseva T, Montessuit S, Martinou J-C, Antonsson B (2002) Bid induces cytochrome c-impermeable Bax channels in liposomes. Biochem J 363:547–552. doi:10.1042/0264-6021:3630547

Sands ZA, Sansom M (2007) How does a voltage sensor interact with a lipid bilayer? Simulations of a potassium channel domain. Structure 15:235–244. doi:10.1016/j.str.2007.01.004

Sanjuan Szklarz LK, Kozjak-Pavlovic V, Vogtle F-N, Chacinska A, Milenkovic D, Vogel S, Durr M, Westermann B, Guiard B, Martinou J-C, Borner C, Pfanner N, Meisinger C (2007) Preprotein transport machineries of yeast mitochondrial outer membrane are not required for Bax-induced release of intermembrane space proteins. J Mol Biol 368:44–54. doi:10.1016/j.jmb.2007.01.016

Schafer B, Quispe J, Choudhary V, Chipuk JE, Ajero TG, Du H, Schneiter R, Kuwana T (2009) Mitochondrial outer membrane proteins assist Bid in Bax-mediated lipidic pore formation. Mol Biol Cell 20:2276–2285. doi:10.1091/mbc.E08-10-1056

Shental-Bechor D, Haliloglu T, Ben-Tal N (2007) Interaction of cationic-hydrophobic peptides with lipid bilayers: Monte Carlo simulation method. Biophys J 93:1858–1871. doi:10.1529/biophysj.106.103812

Sitkoff D, Ben-Tal N, Honig B (1996) Calculation of alkane to water solvation-free energies using continuum solvent models. J Phys Chem 100:2744–2752. doi:10.1021/jp952986i

Sperotto MM, May S, Baumgaertner A (2006) Modelling of proteins in membranes. Chem Phys Lipids 141:2–29. doi:10.1016/j.chemphyslip.2006.02.024

Suzuki M, Youle RJ, Tjandra N (2000) Structure of Bax coregulation of dimmer formation and intracellular localization. Cell 103:645–654. doi:10.1016/S0092-8674(00)00167-7

Tang M, Waring AJ, Hong M (2007) Phosphate-mediated arginine insertion into lipid membranes and pore formation by a cationic membrane peptide from solid-state NMR. J Am Chem Soc 129:11438–11446. doi:10.1021/ja072511s

Terrones O, Antonsson B, Yamagucci H, Wang HG, Liu J, Lee RM, Herrmann A, Basanez G (2004) Lipidic pore formation by the concerted action of proapoptotic BAX and tBID. J Biol Chem 279:30081–30091. doi:10.1074/jbc.M313420200

Valentijn AJ, Upton J-P, Bates N, Gilmore AP (2008) Bax targeting to mitochondria occurs via both tail anchor-dependent and -independent mechanisms. Cell Death Differ 15:1243–1254. doi:10.1038/cdd.2008.39

Veresov VG, Davidovskii AI (2007) Monte Carlo simulations of tBid association with the mitochondrial outer membrane. Eur Biophys J 37:19–33. doi:10.1007/s00249-007-0149-z

Walensky LD, Pitter K, Morash J, Oh K-J, Barbuto S, Fisher J, Smith E, Verdine GL, Korsmeyer SJ (2006) A stapled BID BH3 helix directly binds and activates BAX. Mol Cell 24:199–210. doi:10.1016/j.molcel.2006.08.020

Wei MC, Zong WX, Cheng EH, Lindsten T, Panoutsakopoulou V, Ross AJ, Roth KA, McGregor GR, Thompson CB, Korsemeyer SJ (2001) Proapoptotic Bax and Bak: a requisite gateway to mitochondrial dysfunction and death. Science 292:727–730. doi:10.1126/science.1059108

White SH (2007) Membrane-protein insertion: the biology-physics nexus. J Gen Physiol 129:363–369. doi:10.1085/jgp.200709741

White SH, Wimley WC (1999) Membrane protein folding and stability. Annu Rev Biophys Biomol Struct 28:319–365. doi:10.1146/annurev.biophys.28.1.319

Wimley WC, Gawrisch K, Creamer TP, White SH (1996) Direct measurement of salt-bridge solvation energies using a peptide model system: implications for protein stability. Proc Natl Acad Sci USA 93:2985–2990. doi:10.1073/pnas.93.7.2985

Wolfenden R (2007) Experimental measures of amino acid hydrophobicity and the topology of transmembrane and globular proteins. J Gen Physiol 129:357–362. doi:10.1085/jgp.200709743

Wolter KG, Hsu YT, Smith CL, Nechustan A, Xi XG, Youle RJ (1997) Movement of Bax from the cytosol to mitochondria during apoptosis. J Cell Biol 139:1281–1292. doi:10.1083/jcb.139.5.1281

Yethon JA, Epand RF, Leber B, Epand RM, Andrews DW (2003) Interaction with a membrane surface triggers a reversible conformational change in Bax normally associated with the induction of apoptosis. J Biol Chem 278:48935–48941. doi:10.1074/jbc.M306289200

Youle RJ, Strasser A (2008) The BCL-2 protein family: opposing activities that mediate cell death. Nat Rev Mol Cell Biol 9:47–59. doi:10.1038/nrm2308